THE NOTCHED COATING ADHESION SPECIMEN: A FRACTURE TEST FOR COATINGS AND ACCELERATED SCREENING TEST FOR ADHESION

by

Tsunou Chang

Thesis submitted to the Faculty of the

Virginia Polytechnic Institute and State University

in partial fulfillment of the requirements for the degree of

MASTER OF SCIENCE

in

Materials Science and Engineering

APPROVED:

D. A. Dillard, Chairman

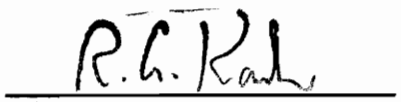

R. G. Kander

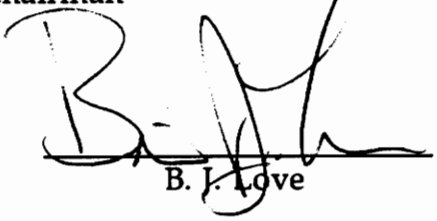

B. J. Love

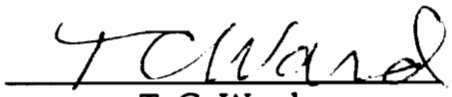

T. C. Ward

May, 1996
Blacksburg, Virginia

THE NOTCHED COATING ADHESION SPECIMEN: A FRACTURE TEST FOR COATINGS AND ACCELERATED SCREENING TEST FOR ADHESION

By
Tsunou Chang
David A. Dillard, Chairman
Materials Science and Engineering

(ABSTRACT)

A simple adhesion test method is proposed to provide estimates of the debond toughness of adhesive bonds. Notched coating adhesion (NCA) specimens consist of single substrates coated with thin layers of adhesive[1]. The coating is notched to induce initial debonds, and the specimen is then loaded in a manner to produce tensile stresses in the coating. The substrate strain at which the coating debond propagates is then used to determine the critical strain energy release rate. Yielding of the substrate is permitted, and does not complicate the calculations. The specimen geometry results in a mode mix which drives the debond to the interface, thus obtaining a measure of interfacial behavior. Because of the geometry and testing method, the technique is simple, inexpensive and may be conducted quickly. The properties of the coating and the residual stresses of the bond must be known to predict the bond strength. Since accurate data on these properties are not always readily available, the test may be limited as a method to screen adhesive systems. Besides being a screening test, the NCA can be used as an accelerated test to study durability of adhesive bonds. NCA specimens reach

moisture equilibrium quickly because of the short diffusion path. By significantly reducing the amount of time needed for the adhesive/substrate interface to reach equilibrium moisture conditions, the time required to obtain estimates of performance in humid environments is greatly reduced. If one assumes that moisture at the interface is the cause of bond degradation, these simple tests offer the potential to rapidly estimate the durability of a given adhesive/substrate system. Accelerated durability studies were conducted on model steel/epoxy systems, and the results were compared to the results for double cantilever beam tests.

ACKNOWLEDGMENTS

I would like to thank Dr. David Dillard for his advice, encouragement and guidance. The long hours he cheerfully invested in this research and in me were greatly appreciated. The help and advice from Dr. Tom Ward, Dr. Ron Kander, Dr. Brian Love and Dr. John Dillard are also acknowledged.

Thanks also go to the Center for Adhesive and Sealant Science, the Dow Chemical Co. and the National Science Foundation for supporting this research.

I would like to acknowledge the help of Dr. Nick Shephard, Dr. Yeh-Hung Lai, Mr. Raúl Andruet, Mr. Dwayne Rakestraw, Ms. Elizabeth Sproat and Ms. Holly Gurbacki for all the hours they put into this research. Thanks also go to all the members of the Adhesion Mechanics Laboratory for their support and comments.

My special thanks and a hug to Feyza for the moral support, the laughs and all the valuable suggestions she made for this research.

Finally I would like to thank my family for all the support they gave me. Without them, I would not have been here.

TABLE OF CONTENTS

LIST OF TABLES

LIST OF FIGURES

α	Dundurs' parameter α
a	Initial debond length
ASTM	American Society for Testing and Materials
B	Specimen width
CTE	Coefficient of thermal expansion
Δ	Crosshead deflection
D	Diffusion constant
DCB	Double cantilever beam
Dicy	Dicyandiamide
DSC	Differential scanning calorimetry
E	Modulus of the coating
E_S	Modulus of the substrate
ε	Tensile strain
G_C	Critical strain energy release rate
G_I	Strain energy release rate (mode I)
G_{II}	Strain energy release rate (mode II)
G_{Ic}	Critical strain energy release rate (mode I)
G_{IIc}	Critical strain energy release rate (mode II)
GPa	Giga Pascals
h	Coating thickness
h_c	Critical thickness of the coating
H	Substrate thickness
I	Moment of inertia
IC	Integrated circuits
K	Fracture toughness
LaRC	Langley Research Center
LDPE	Low density polyethylene
LEFM	Linear elastic fracture mechanics
M_t	Mass of the polymer at time t
M_∞	Mass of the polymer at time infinity
ν	Poisson's ratio
NCA	Notched coating adhesion
P	Load
PVC	Polyvinylchloride
PDMU	3-Phenyl-1,1 dimethyl urea
PEEK	Poly-ether ether ketone
PWB	Printed wire board
rpm	Revolutions per minute
RH	Relative humidity

SERR	Strain energy release rate
SLJ	Single lap joint
σ	Tensile stress within the coating
σ_m	Moisture swelling stress
σ_{max}	Maximum stress of the polymer
σ_t	Thermal residual stress
t	Time since humidity conditioning
T_e^c	Critical fracture efficiency parameter
T_e	Fracture efficiency parameter
Tg	Glass transition temperature
TMA	Thermal mechanical analysis
ω	Loading angle
x	Apparent crack length offset
Z	Dimensionless driving force

1.0 INTRODUCTION

As structures and structural materials become lighter, conventional joining methods such as rivets and bolts impose a significant weight penalty. Engineers, scientists and designers are faced with the problem of finding better methods to efficiently join these materials. Adhesives have become an attractive alternative because they result in light-weight and efficient structures without weakening the adherends to the extent experienced with conventional joint methods. For example, an aircraft that incorporates all current adhesive technologies can save up to 5 percent of its weight[2]. Adhesives not only reduce the weight of a structure, they can also resist fatigue, damp vibration and defy corrosion better than conventional joints[3].

Another important field for adhesive applications is in microelectronics, the mainstream of the electronics industry. Today, integrated circuits (IC) and printed wire boards (PWB) are more intricate than ever. Many times, these chips and boards are protected by films and coatings, and many metal film circuits are adhesively bonded to plastic boards. The coatings, films and adhesives are exposed to constant thermal and environmental attacks. Improving bond performance and durability over the lifetime of the equipment is a formidable task, but it might provide rewards such as smaller, longer lasting and more powerful chips and IC's[4].

With the potential advantages, the use of adhesives can no longer be ignored. Research is being conducted to answer many questions that arise with the use of adhesives. Unfortunately, many experiments used to characterize adhesive performance and durability are time consuming and costly. The single lap joint (SLJ) specimen, for example, is easy to fabricate and test, but is quite complicated to analyze for accurate results as Goland and Reissner[5] and many others have demonstrated. Double cantilever beam

(DCB) specimens are more complicated to test and fabricate but easier to analyze. The failure mode of all these tests can be either cohesive or interfacial, and there is no guarantee which one will occur[6]. There are many other tests designed for adhesive durability and debond toughness studies, some of which are discussed in Section 2.0.

This thesis proposes an alternate test geometry for screening adhesive systems and accelerating humidity conditioning of adhesive systems. The notched coating adhesion (NCA) test may prove to be ideal for screening adhesive systems because it yields quantitative results quickly and inexpensively. Being a coating specimen, the test can be used to test the performance of films and coating systems. When used for durability studies, the NCA test is based on the observation that failures resulting from long term exposure to humid conditions tend to be interfacial[7-8]. A further assumption is that the presence of moisture at the interface leads to a rather rapid degradation in interfacial strength. Thus, if the time required for the interfacial region to saturate with moisture is reduced, the time required to measure the degraded strength can also be reduced. While there may be some adhesive/substrate systems which are not appropriately modeled by these assumptions, the approach is believed to be appropriate as a preliminary screening tool for many systems of practical interest. The acceleration in conditioning is achieved by testing the adhesive as a coating bonded to a single substrate rather than as an adhesive bonding two substrates together. Being an inherently interfacial failure test, the experiment method may also be a good candidate for surface studies such as surface treatment effects on adhesive systems.

2.1 Currently Used Coating Tests

A number of specimens have been proposed and utilized for testing coating adhesion. Besides being used to study coatings, many of these testing methods are widely used in the adhesive industry for screening new adhesive systems. Some of the coating adhesion tests are: the scratch indentation test[9], the pull-off test[10], the self delamination test[11], the peel test[12-14], the cross-hatch tape test[15], the interlaminar bond strength test[16] and the blister test[17-18].

In the scratch indentation test[9], a probe indents the film at a prescribed load. This probe is then dragged across the specimen, and the load required to scrape the coating from the substrate is recorded. In a comparative test, a coating that requires a higher load to produce debonding is normally assumed to have a better bond than the one requiring a lower load. Although useful for testing coatings, the results are difficult to interpret quantitatively. For the scratch indentation test, a special setup must be fabricated to monitor the load required to drag the probe. The moving indenter creates shear stresses in the substrate and the coating; furthermore, many researchers have demonstrated that friction may affect the critical normal force required to move the probe[19-20].

Several pull-off test techniques have been proposed. These tests are based on bonding a stud to a coating, and then pulling the stud in tension to determine the load required to debond the coating[10]. A low temperature adhesive is normally used for bonding the stud to prevent the heat from damaging the coating. In case where these tests are used for durability studies, the stud curing process should be fast enough so that the moisture content remains nearly unchanged. For each test to be successful, the adhesion of the coating to the substrate must be weaker than the adhesion of the stud to the

coating; otherwise, the stud debonds instead of the coating. Because these are maximum strength failure tests, the debond is generally catastrophic, and the failure stress for bonds can be determined.

The cross-hatch tape test, ASTM D 3359[15], is a widely used test in the industry. It involves using a knife to cross-hatch a coating. A pressure sensitive adhesive tape is then applied to the cross-hatched region and peeled away from the substrate. Coating adhesion is qualitatively determined from the number of coating fragments remaining on the substrate. Use of this method after humidity conditioning is widespread, but the test is subjective and it cannot be easily reproduced. For durability studies, a failure to account for changing adhesion between the pressure sensitive tape and the exposed coating surface may result in inconsistencies.

The peel test is another extensively used test to study coating and film adhesion. In the peel test, a thin flexible strip bonded to a substrate by a layer of adhesive is pulled away from the substrate at a predetermined angle. The peel force can be recorded, and the strain energy release rates may be determined. Analytically, substrate yielding or bending are normally assumed to be negligible except in T-peel test where substrate yielding must be considered in the analysis. The test is also highly dependent on strain rate, thickness of the coating, and the loading angle[12-14].

In the self delamination test developed by Farris and Bauer[11], a small hole is drilled through the coating. Because of the peel and shear stresses, debonding occurs around the hole. The strain energy release rate can be determined from the size of the debond around the hole. The test uses a fracture mechanics approach and can be used to determine bond toughness quantitatively.

The interlaminar bond strength test developed by Cropper and Young[16,21] is in many ways similar to the NCA test. The test was developed

for the measurement of interlaminar bonding strength, and so far has been demonstrated to be useful for laminates composed of polypropylene copolymer (PP) film , aluminum foil and polyester. The specimen is similar to a tensile test, but the specimen has a groove through the polyester/aluminum layers.

To determine the strain energy release rate, it is necessary to determine the properties of the non-laminated PP film. The load-displacement curves for both laminated specimen and PP material have a peak load as the yielding is initiated, followed by a plateau load as the yielded area propagates. If the plateau loads of PP film and the laminate are $\mathbf{P_{0pp}}$ and $\mathbf{P_b}$ respectively; $\mathbf{X_f}$ is the final displacement, and **A** is the original laminate area, the overall strain energy release rate (**G**) can be found to be:

$$G = \frac{X_f}{A}\left(P_b - P_{0pp}\right) \qquad (1)$$

The testing method requires that both the load and displacement data and the mechanical behavior of the substrate to be known. If the load does not reach a plateau, other types of analysis are required. In the NCA test, the loading values are not necessary and strain energy release rate is determined from the values collected at the moment debond propagates; while in the interlaminar bond strength test debond is required, but bond energy is determined by the plateau loads of the bulk PP film and the laminate.

Originally proposed by Dannenberg[18], various types of blister tests have been developed for testing flexible coatings. Basically, blister specimens consist of a film bonded to a rigid substrate with an initial debond where pressure can be introduced. When pressure is applied through the debond, the film flexes and forms a blister. The pressure that causes debond, the size of the debond as well as modulus and geometry etc. are used to determine strain energy release rate[17]. The blister test causes uniform stress distribution

in film adherends and it is quite compatible with durability studies "because the pressurizing medium is contained within the blister region[17]". The test however, usually does not work well with brittle coatings. Many types of well developed blister geometries are available, each with different characteristics. Some of these types include the standard blister, the island blister, the peninsula blister and the constrained blister. Lai and Dillard[22] wrote a comprehensive paper comparing the different types of the blister tests.

2.2 The Importance of Durability Studies

The ability to determine the durability of adhesive bonds remains an elusive task, especially when the service environment involves exposure to diluents such as water. Moisture continues to be of major concern for many adhesive bond systems for a number of reasons including:

1) many adhesives are hydrophilic, picking up significant amounts of moisture over time changing mechanical properties of the adhesion;
2) most adhesives and some adherends allow moisture permeation, eventually reaching the adhesive/adherend interface;
3) the high surface energies of metallic and certain other substrates result in moisture migrating to the adherend surfaces and, in some cases, displacing the adhesive from the substrate, oxidizing the adherend, etc., and
4) absorbed moisture induces swelling stresses which can reduce the bond strength.

Recognition of this susceptibility to moisture has led to extensive studies aimed at evaluating the effects of moisture, developing an understanding of the responsible mechanisms, and predicting the performance of adhesive bonds subjected to humid environments. While some studies have focused

on the effect of humidity on neat adhesive samples, most studies have recognized the significance of the adhesive/adherend interactions, and have evaluated strength of actual bonded joints. Unfortunately, the time required for typical bonded geometries to reach moisture equilibrium can be quite long. Single lap joints (SLJ) and double cantilever beam (DCB) specimens with a width of 25.4 mm may take up to several years to equilibrate, depending on the temperature and adhesive. Such lengthy conditioning times hamper the development of improved adhesives, and may delay the acceptance of these adhesives because of the time required to certify them. Reliable methods to accelerate the durability testing of specimens would be of significant benefit to adhesive formulators and users.

Currently, one commonly used method for accelerated testing of adhesive strength is by conditioning DCB or SLJ specimens at high temperature and high humidity levels[7,23-24]. The high temperature can increase the diffusivity, thus decreasing the time required to saturate the specimens. Use of increased temperature to accelerate humidity conditioning, however, raises concerns about whether the elevated temperatures are introducing anomalous damage modes. Placing specimens in boiling water is a routine practice to screen specimens, and yet extrapolating results from this accelerated conditioning process to durability in service conditions is questionable. Furthermore, the conditioning time under these elevated temperature conditions may still be rather long considering that the moisture has to diffuse through the edges.

Another popular accelerated testing method is the wedge test[25-26]. After the wedge is driven into a bonded specimen, the loaded specimen is placed into a water bath or environmental chamber. Over time, the debond may propagate, reducing the stresses imposed by the wedge. Although the moisture state is not well understood ahead of a propagating debond, the

adhesive does become saturated ahead of a slow growing or equilibrated debond. Results are frequently given as debond length as a function of exposure time, although the critical strain energy release rate can be calculated from this testing method.

It has been established that the interphase is often the region most susceptible to moisture attack[7], the knowledge of environment degradation on the interface is essential for predicting the long term performance of adhesively bonded structures. Assuming the interphase of specimens in which the adhesive is used as a coating bonded to a single substrate is identical to the interphase of the adhesive and the two substrates in sandwiched specimens (*e.g.*, double cantilever beam), then one can study the interphase degradation due to moisture with coating adhesive specimens to predict durability rather than specimens with adhesive bonding two substrates together. The advantage to the coating approach to study moisture effects is that water diffuses into the adhesive through the top of the specimen so that the time required to saturate the adhesive and the interphase is shorter. For a full treatment on diffusion and durability refer to Section 4.0.

2.3 The Use of Notched Coating Adhesion Test to Study Durability

The NCA test may be a good test for accelerated durability and the interface studies due to its geometry and loading mode. Conventional sandwiched adhesive specimens like the ASTM D3433 standard DCB specimen[27] consists of an adhesive sandwiched by two substrates and only the edges of the adhesive are exposed. If a DCB specimen is environmentally conditioned, water can diffuse into the adhesive only through the edges (assuming that the adherends are not permeable, and no wicking is present).

Thus, the diffusion path is half the specimen's width (Fig. 1b). To reduce the conditioning time, one can either increase the diffusion coefficient or decrease the diffusion path. A common method to increase diffusion coefficient is by increasing the conditioning temperature. However, the possibility of introducing spurious degradation modes exists.

The use of NCA specimens can drastically decrease the required conditioning time to reach moisture saturation by decreasing the diffusion path. An adhesive coated to a single substrate offers the advantage of a short diffusion path since the diffusion path is the thickness of the adhesive coating (Fig. 1b). The NCA test takes advantage of the short diffusion path in order to accelerate humidity conditioning and estimate the bond durability. Many times, solvent diffusion through polymers can be considered to behave in a Fickian manner; therefore, the time required to saturate specimens increases with the square of the diffusion distance (Fig. 1).

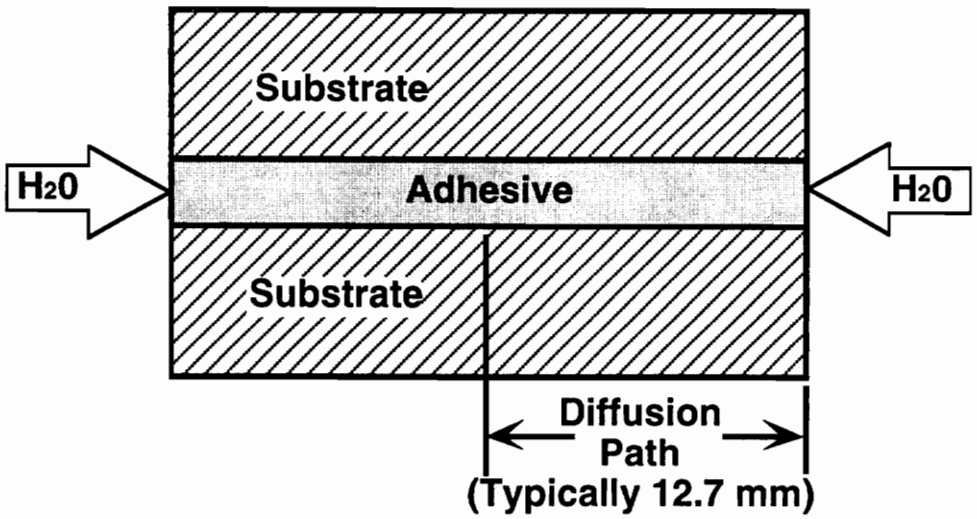

Figure 1a. Cross section of a sandwiched specimen. The diffusion path is equal to half of the width.

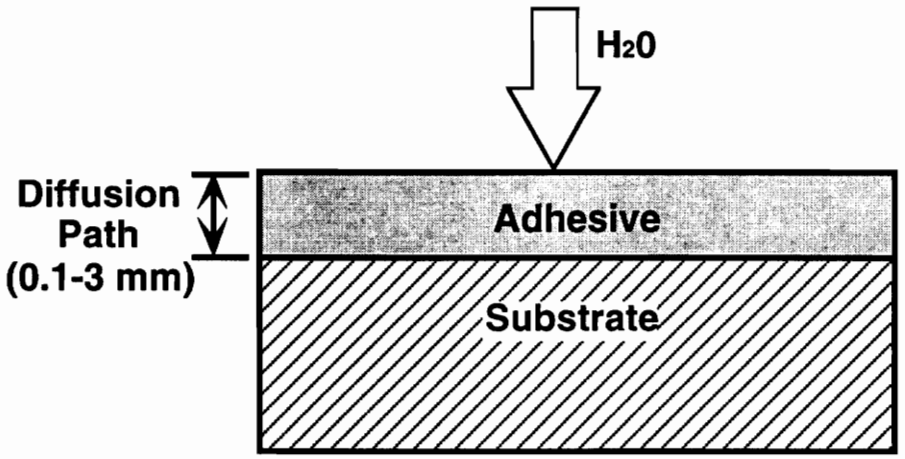

Figure 1b. Cross section of a coating specimen. The diffusion path is equal to the thickness.

3.0 THE NOTCHED COATING ADHESION TEST

The proposed notched coating adhesion (NCA) specimen consists of a coating layer bonded to a single substrate as illustrated in Figure 2. A notch is introduced into the coating near the center of the specimen. When properly introduced, the notch creates enough stress to locally debond the coating; thus, producing two sharp tipped cracks along the interface. The length of the local debond is named **a**. Using an axial loading device, the specimen is loaded in tension perpendicular to the cut (Fig. 2-3). The stress state generated causes the debonds to propagate. Being a constant strain energy release rate specimen, the debond propagation does not alleviate the applied strain energy, thus, the resulting debonding is often quite rapid and easily observed. The critical strain (ε_c) at which the debond starts to propagate is recorded to determine the critical strain energy release rate ($\mathbf{G_c}$).

3.1 Fracture Testing

Many technical advances have been made on understanding adhesive systems' performance in the past few decades. One of the successful tools which has been used to evaluate adhesive systems' performance is fracture mechanics. Due to its success in the past, fracture mechanics has served as the testing and the analysis foundation of the NCA research and development.

The existence of flaws and cracks cannot be ignored in any type of structure. At the same time structures are required to be safer than ever before. Consequently, accurate quantitative measures of material tolerance to cracks and flaws must be determined. Since part of the definition of fracture mechanics is the requirement of a dominant crack in the structure, the testing method is especially attractive to designers of many types of structures.

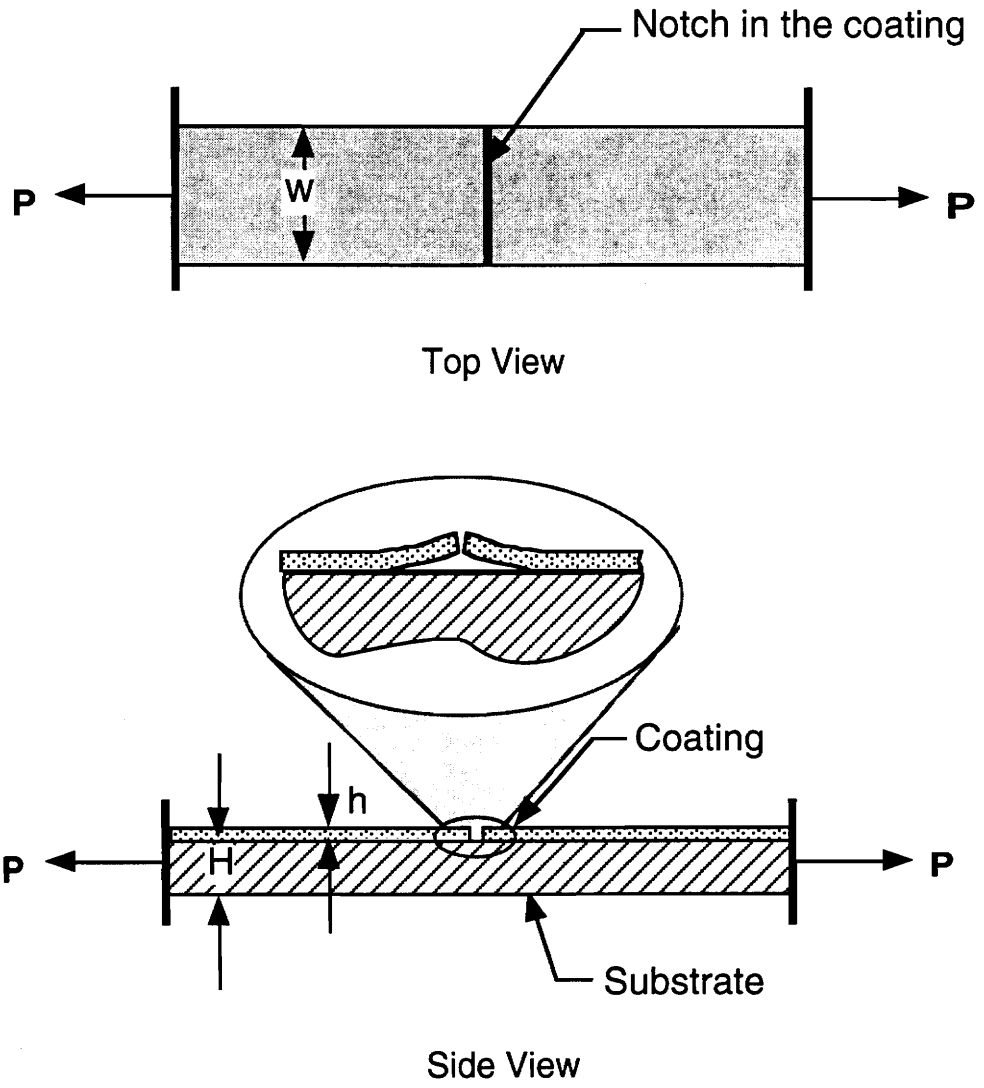

Figure 2. Top and side views of the notched coating adhesion (NCA) specimen.

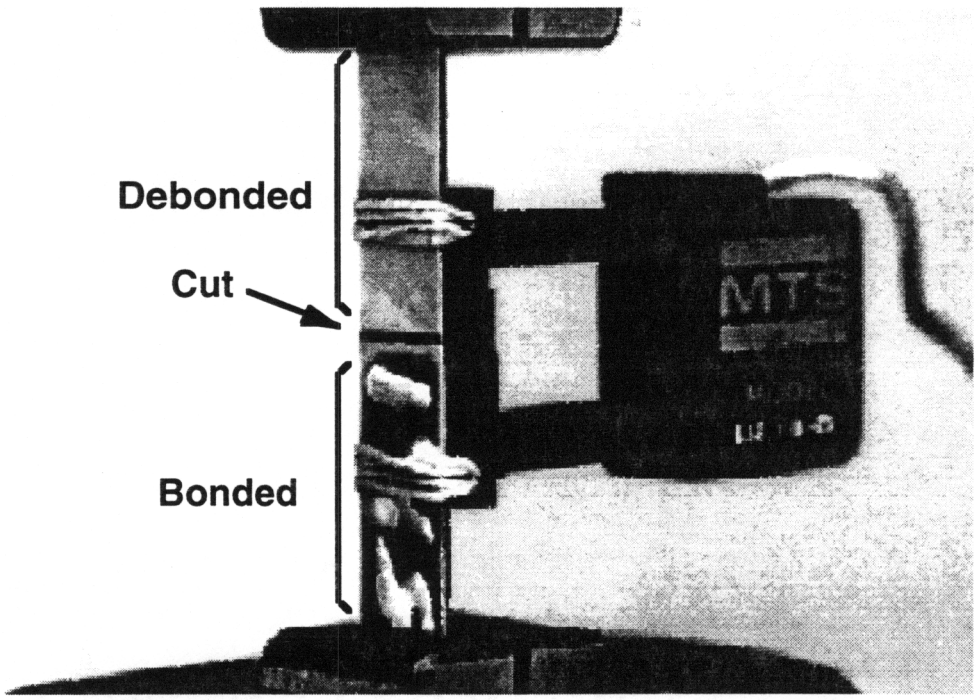

Figure 3. NCA test in progress. The upper part is debonded and the lower is on the verge of debonding. Note the initial debond below the cut. (The white markings on the lower part of the specimen are for labeling purposes).

A drawback to fracture mechanics is that the fracture properties cannot be directly measured; the fracture properties must be inferred from quantities that can be determined experimentally. Fracture mechanics was chosen as the framework for the new specimen design because fracture test results generally can be easily used to predict the bond toughness of other adhesive joints. As a result, these fracture mechanics based tests make it possible to gain more fundamental understanding of the failure mechanisms of the adhesive systems being studied. Fracture mechanics also has an extrapolative function. Small-scale laboratory tests can be utilized to predict the properties of a large-scale structure. Therefore, this fracture mechanics testing approach should also provide more meaningful data for design of engineering structures which realistically contain flaws.

Fracture tests apply the concepts of either stress intensity factors or strain energy release rates. The NCA study utilizes the strain energy release rate, which uses an energy balance approach to analyze and describe crack growth phenomena. The values for the strain energy release rate are used as an indication of the loading level being applied to the crack tip of a specimen. The symbolic notation used for the strain energy release rate is **G** with subscripts used to denote whether the **G** is critical ($\mathbf{G_C}$) or applied total strain energy release rate (**G**). The total loading stress is referred to as the total applied strain energy release rate (**G**). The critical strain energy release rate ($\mathbf{G_C}$) is a material system's property. $\mathbf{G_C}$ is the amount of energy required for crack growth. This energy can be applied by external load and internally stored energy such as residual stress. In adhesive systems, $\mathbf{G_C}$ can be a function of many variables such as interphase properties, adhesive and substrate properties, specimen dimensions, loading rate, mode mix and environmental conditions.

In linear elastic fracture mechanics (LEFM) both G_C and G can be broken into three primary modes of loading. They are: the opening or tensile mode(G_I), the sliding or shear mode (G_{II}) and the tearing or antiplane mode (G_{III}) (Fig. 4). In many shear type joints, mode II is normally the predominant loading mode accompanied by some mode I. In adhesive test geometries however, mode I testing seems to be the trend. Since specimens tend to be weakest when loaded in mode I, these test results tend to be conservative. For more information on fracture mechanics, refer to Broek[28], and Kanninen and Popelar[29].

3.2 Specimen Fabrication and Testing

There are two typical methods to fabricate NCA specimens. Many times, the choice of the technique depends on the type and the quantity of the desired testing system. The two procedures differ in the order of the required steps. One fabrication method is to bond large panels and then cut individual specimens from the panels. The other method is to cut specimens to the proper size and then bond the coating on the substrate. In the first method, the size of the panel is limited by the number of specimens required, the size of the oven or hot press, and the availability of the substrate and the coating. The substrate and the coating are prepared and bonded with the prescribed technique. After cure, the edges can be removed since they tend to have non-uniform thickness. The rest of the panel can then be cut or sliced to appropriate test dimensions.

For coatings that flow during cure, a dam can be placed on the edges of the panel. The dam holds the coating in place and it also serves as a means to control the thickness of the coating. The dam can be formed with strips of

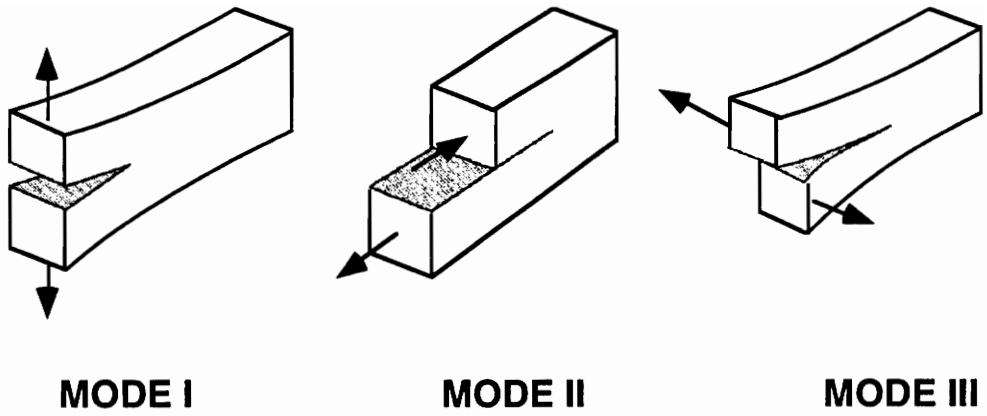

Figure 4. Possible fracture modes.

Teflon or other convenient materials. A small space can be left on the sides of the strips to allow for polymer overflow. This method ensures that all specimens fabricated from the same panel are virtually the same with a uniform coating thickness. The disadvantage is that the cutting process may induce undesirable stresses or debonds in the specimens.

The second method is to perform the appropriate curing process after cutting substrates and possibly coating (if it is a film before cure) to testing sizes. If the coating flows during cure, dams must be setup around the specimens to generate the desired uniform thickness. This method is advantageous when limited specimens are needed, and since the specimens are cut before cure, the cutting process does not induce any stresses. However, great care must be given to minimize problems associated with spewing of the polymer, edge effects, control of thickness, etc.

After fabrication, the specimen geometry is carefully measured. Measurements include the width and length of the specimen and the thickness of both the coating and the substrate. These measurements are required for the analysis described in the next section. There are some limitations to the acceptable NCA dimensions. To simplify analysis, the substrate's thickness should be large enough so that residual stresses will not cause any bending of the specimens. For the equipment used for the experiments cited in this paper, it was found that specimens with 120 mm by 12.7 mm dimensions worked best. About 40 mm of each end is used for gripping, making the effective testing section 80 mm by 12.7 mm. A 25.4 mm gage length extensometer was used to monitor strain (Fig. 3). The width of 12.7 mm was chosen since it fits the 25.4 mm wide grips well, and it has the same width as the extensometer used. The thickness of the substrate and the coating is a function of the system being studied. The thickness depends on the strength of the bond, the yielding and the breaking stresses of both the

substrate and the coating and the feasibility in fabrication. The analysis section (Section 3.3) gives more detail on choosing the right thickness.

The notch to generate the initial debond is an important part of the test. Care must be taken so that the coating is cut through and that initial debonds are generated every time. This initial debond is the flaw required in fracture mechanics. For soft adhesives a sharp razor blade can be used as the cutting device. The blade is tapped into the adhesive perpendicular to the loading direction in the middle of the specimen. Frequently, the stresses imposed by the blade causes the adhesive to debond locally near the cut (Fig. 5); thus, producing sharp tipped cracks propagating along the interface[30]. By varying the tapping force, the length of this initial debond can be affected. An initial debond length (**a**) of up to five times the coating thickness (**h**) is needed for the NCA test to be perfectly valid. Past experience has demonstrated that producing a debond length exceeding five times the thickness is usually a relatively easy task. The actual **a** to **h** ratio is a function of the adhesive being studied. The reasons for this measure and methods to determine the correct ratio are explained in the next section. For stiff coatings, a coping saw may be used to cut the coating in half. Then, a razor blade can be used to push the edges of the cut to generate the initial debond. Note that for a single notch, there are two debonds which can propagate resulting in two critical strain readings. If a specimen is long enough, several notches could be applied to obtain several critical strain data.

The specimen can be tested with any type of loading device that produces tensile forces. No load cell is required since load is not part of the strain energy release rate equations derived. An extensometer is attached to the substrate of the specimen as shown in Figure 3 to monitor strain. Strain gages can also be used for this purpose. The authors normally test NCA

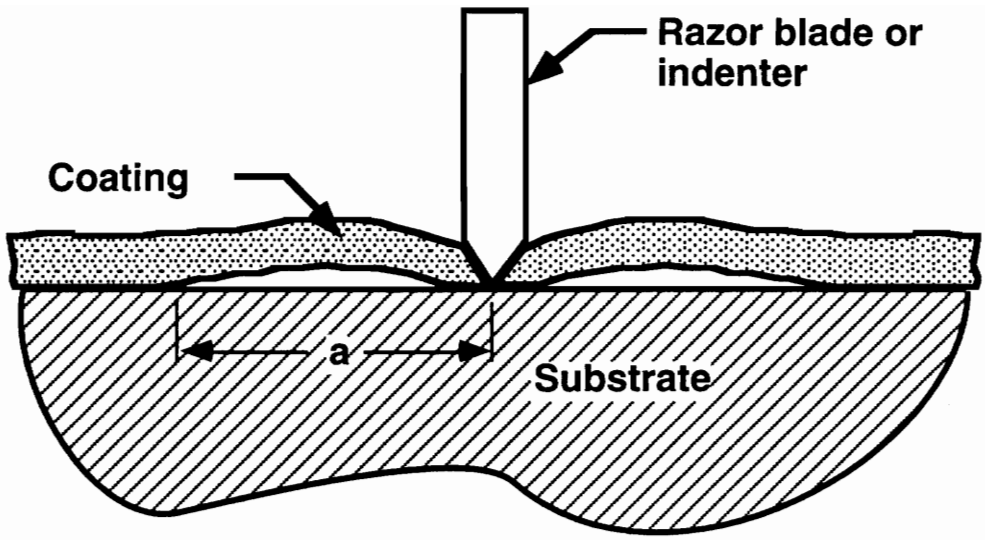

Figure 5. The generation of the cut and the initial debond.

specimens at a rate of 10 mm/min. Other loading rates ranging from 1 up to 15 mm/min. were also used without any difficulty. It is predicted that loading rate will affect the results obtained, but since the current research does not involve viscoelastic studies, there was no attempt to correlate the loading rate with G_c. At the critical strain, the debond rapidly propagates to the end of the specimen. If an extensometer is used, and if it is attached to the specimen with rubber bands, cracks might propagate rapidly and then stop where the rubber bands are located. Generally, the crack propagation can be observed easily; since the coating is usually thin, it tends to bend, and the color tone tends to change when debond propagation occurs.

3.3 Specimen Analysis

NCA specimens are strikingly similar to cracked lap shear (CLS) specimens first proposed by Brussat et. al.[31]; in appearance, NCA specimens look like two CLS specimens attached end to end (Figure 6). The mode mix of NCA specimens is also similar to CLS specimens. Many times, the analysis of CLS specimens must be treated as a geometrically nonlinear problem due to the large rotations[32-33]. Because of the thin coating on a thick substrate for the NCA specimen, rotations can generally be assumed to be negligible; therefore, NCA analysis is considerably simpler than CLS analysis. Both analytical solutions and finite element methods were used to analyze the NCA test geometry. In many studies, the solutions from the two methods of analysis were compared.

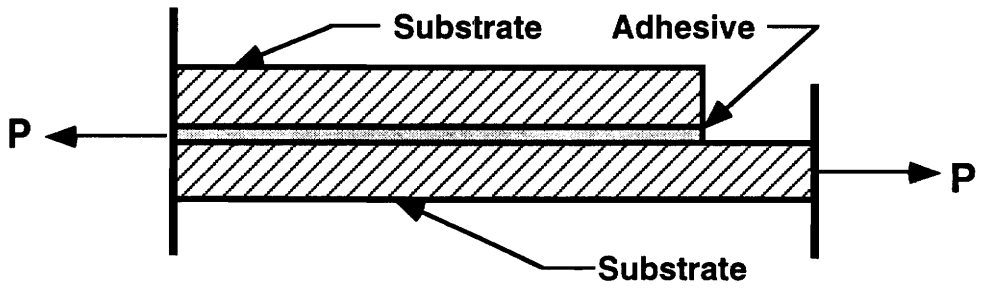

Figure 6a. Schematic of the cracked lap shear specimen.

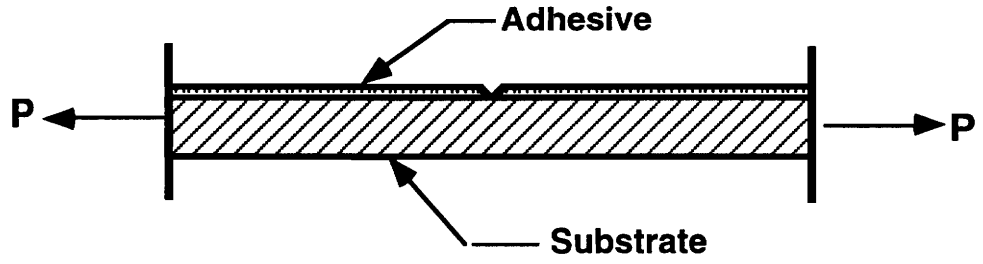

Figure 6b. Schematic of the notched coating adhesion specimen.

3.3.1 Analytical Methods

For investigating NCA analytically, uniform stresses and modulus through the thickness of the coating were assumed. The analysis also assumes the substrate to have a very large bending stiffness compared to that of the coating. For any coated materials, the strain energy release rate for the coating can be expressed as[34]:

$$G = \frac{Zh\sigma^2}{\hat{E}} \tag{2}$$

where Z is the dimensionless driving force;

σ is the tensile stress within the coating;

h is the coating thickness, and

$\hat{E}$ is the effective modulus of the coating.

$$\hat{E} = \begin{cases} E & \text{for plane stress} \\ \dfrac{E}{(1-\nu^2)} & \text{for plane strain} \end{cases}$$

ν is Poisson's ratio, and

E is the tensile modulus of the coating.

For debonds like the ones encountered in NCA specimens, **Z** is a function of the initial debond length (**a**), coating thickness (**h**) and the Dundurs' parameter α. Dundurs defined α as[34]:

$$\alpha = \frac{\hat{E} - \hat{E}_s}{\hat{E} + \hat{E}_s} \tag{3}$$

where $\hat{E}_s$ is the effective modulus of the substrate.

At short crack lengths, as **a/h** approaches 0 and α approaches 1, **Z** approaches infinity. If α approaches -1, then **Z** approaches 0. However, for any system, when crack debond is many times longer than the coating thickness (steady state), **Z** approaches 0.5[34]. The analytical solutions consider

the crack length to be at its steady state therefore **Z** is assumed to be 0.5. Many researchers suggest that **a/h** > 5 is a good assumption for **Z** to be considered constant[34]. In the finite element work (Section 3.3.2) the effect of crack length and coating thickness on **Z** and G_C are studied.

The assumption of steady state crack propagation means that the debond is propagating in a self-similar manner with a straight debond front. This requires that the initial debond be several times longer than the coating thickness in order to have self-similar propagation. If the debond length is long compared to the width, the plane stress modulus should be used. For shorter crack lengths, the behavior can approach plane strain conditions. Under other conditions, neither solution is expected to be exactly valid, but they would narrowly bracket the actual solution. For NCA test analysis, equation (2) must be modified to account for the residual stresses due to curing. Note that the residual stress is assumed to be an equal biaxial stress and that loading is assumed to be uniaxial. The specimen is assumed to be infinitely long; the thickness and moduli of the coating and the substrate were taken into account in the same manner as Brussat *et. al.* did for the CLS analysis[31]. This correction is an approximation derived form the energy balance equation. The mixed mode (mode I and II) strain energy release rate for the NCA may be determined as:

$$G = \frac{h}{2\hat{E}}\left[\left(\sigma_t + \varepsilon\hat{E}\right)^2 + \left(\sigma_t - \upsilon\varepsilon\hat{E}\right)^2\right]\left[1 + \frac{h\hat{E}}{HE_s}\right] \qquad (4)$$

Where σ_t is residual biaxial stress due to cooling after high temperature cure,

ε is applied uniaxial tensile strain, and

H is the thickness of the substrate.

If the NCA test is used to study durability of adhesive joints, Equation (4) must be modified to account for the physical changes that occur during specimen conditioning. New stresses may be generated; these include stresses

caused by the swelling of the polymer due to moisture ingression, and thermal loading. Tests are required to determine the saturated adhesive modulus dependence on conditioning temperature and humidity. Appropriate terms must be added to Eq. (4):

$$G = \frac{h}{2\hat{E}}\left[\left(\sigma_t + \sigma_m + \varepsilon\hat{E}\right)^2 + \left(\sigma_t + \sigma_m - \upsilon\varepsilon\hat{E}\right)^2\right]\left[1 + \frac{h\hat{E}}{HE_s}\right] \qquad (5)$$

Where σ_m is the residual biaxial stress due to moisture swelling at a given humidity level, and the moduli are now the saturated moduli of coating and substrate.

If the substrate is many times thicker than the adhesive and/or if the substrate is many times stiffer so that $\frac{h\hat{E}}{HE_s} \approx 0$, then the substrate can be considered infinitely stiff (Dundurs' parameter $\alpha \approx -1$), and the contribution to the strain energy release rate can be ignored. For typical coating systems, this is often the case; therefore, Eq. (5) can be simplified to:

$$G = \frac{h}{2\hat{E}}\left[\left(\sigma_t + \sigma_m + \varepsilon\hat{E}\right)^2 + \left(\sigma_t + \sigma_m - \upsilon\varepsilon\hat{E}\right)^2\right] \qquad (6)$$

Equation (6) takes into account the overall strain of the specimen, and the mechanical characteristics of the substrate can be ignored. One advantage to this is that the substrate can deform plastically without causing any significant effect on the results. More analysis on the substrate effects are reported in the finite element section of the thesis.

If the coating deforms plastically, and assuming that the slope of unloading of the coating is the same as the loading modulus, the analysis does not become considerably more difficult. Unlike the peel test analysis with gross yielding, which requires the determination of the plastic energy dissipation, there is no need to consider this term when deriving the energy release rate for the NCA test because the energy spent to yield the coating is

stored after debond, and the equations do not include this energy. Although a coating may yield during the loading process, the unloading of the material after fracture at the debonded portion is always elastic. Therefore, to determine the energy release rate in the NCA test when the coating yields, the fracture energy is simply equal to the elastic strain energy released during the unloading process (Fig. 7). If we break the total strain into two components: plastic strain(ε_p), and elastic strain (ε_e), and replace the ε by ε_e in equations (4) to (6), the plastic deformation of the coating is corrected.

The NCA specimen can be modeled as a layered bi-material where the coating is a very thin layer on top of a thick substrate. To determine the contribution from each fracture mode in the strain energy release rate obtained, Hutchinson and Suo's[34] layered bi-material analysis is applied. The mode mix is a function of the angle ω[34]:

$$\frac{G_{II}}{G_I} = \tan(\omega)^2 \qquad (7)$$

Where ω is a function of Dundurs' parameters α and β[34]; that is, the mode mix is a function of the material mismatch parameters. Values for ω can be found in Suo and Hutchinson's paper[36]. For typical adhesive systems, ω ranges from 40° to 70°; the preferred failure direction for this range is directed towards the interface. An inherent characteristic to this type of mixed mode fracture test is that there is an incentive for the coating to fail in the interface (Fig. 8). All specimens tested to date, which included various adhesive systems had failures that appeared (visually) to be interfacial.

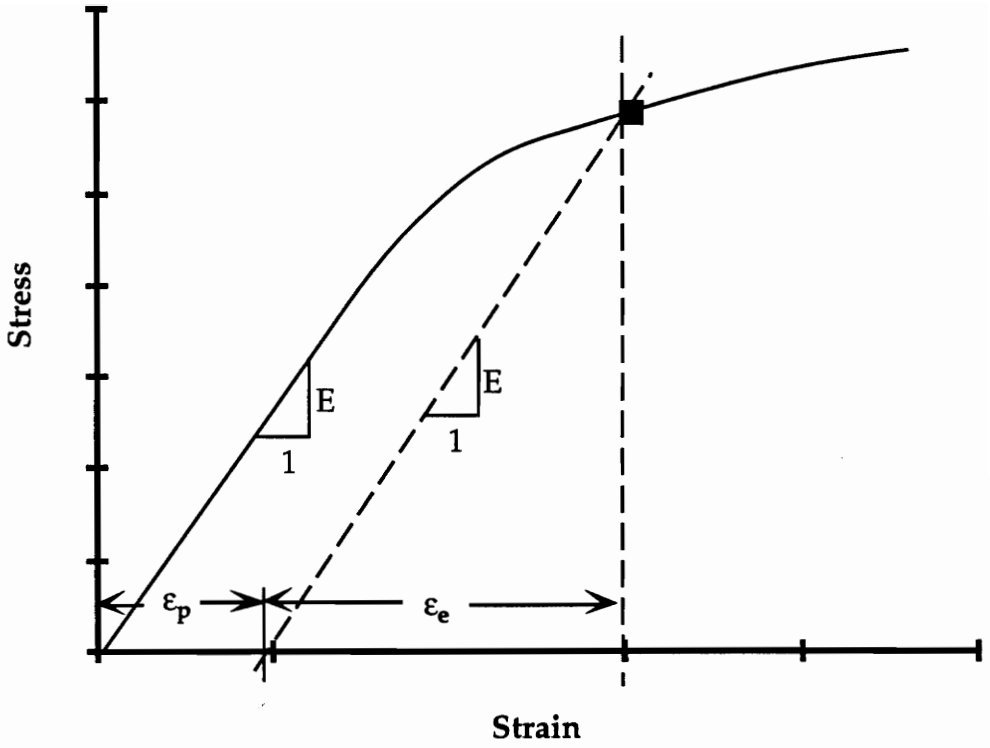

Figure 7. Elastic and plastic strain of stress-strain curve.

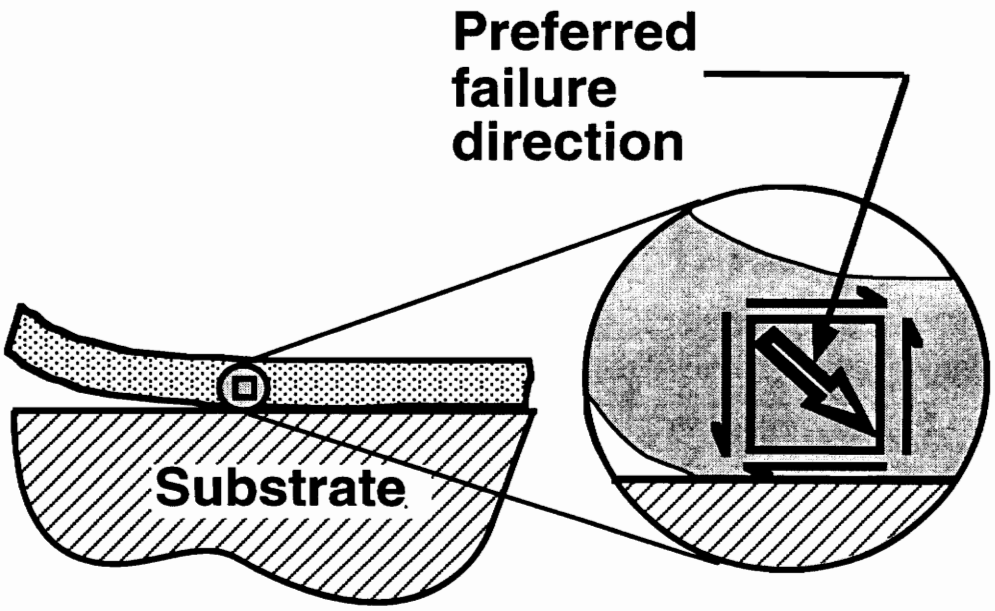

Figure 8. Interfacial failure of NCA specimens.

If plastic deformation of the coating is not desired, methods are developed to avoid it. For plastic deformation analysis, the authors used the fracture efficiency concept proposed by Lai and Dillard[37]. The fracture efficiency parameter ($\mathbf{T_e}$) is defined as the ratio between the energy release rate and the square of the maximum non-singular stress. This means that $\mathbf{T_e}$ is a measure of the test's ability to produce a maximum strain energy release rate at a given stress level (Eq. 8).

$$T_e = \frac{G}{(\sigma_{max})^2} \tag{8}$$

By designing a specimen with a high fracture efficiency parameter, the debonding is more likely to occur without yielding, and therefore allows the elastic analysis to be used. The NCA test can be assumed to be a zero degree peel test, the moment approaches zero, and fracture efficiency parameter becomes:

$$T_e \approx 0.5\frac{h}{\hat{E}} \tag{9}$$

Note that this is the highest $\mathbf{T_e}$ that can be obtained in any type of adhesive bond fracture test[37]. This means that it is possible to obtain very high strain energy release rates at small stresses compared to other tests such as the blister test or the wedge test[37] (Figure 9). Note that although the CLS test is similar to the NCA test, its fracture efficiency is noticeably lower. This is due to the fact that in the simple analysis of the CLS test, neither the substrate nor the adhesive are allowed to yield while the substrate of the NCA tests is allowed to deform plastically. The advantage of the high $\mathbf{T_e}$ is that the coating can be made thinner without causing yielding. A thinner coating helps in accelerating the specimen for durability studies as explained later (Section 4.0). Note that if the NCA specimen's coating yields, it does not change the fracture efficiency parameter.

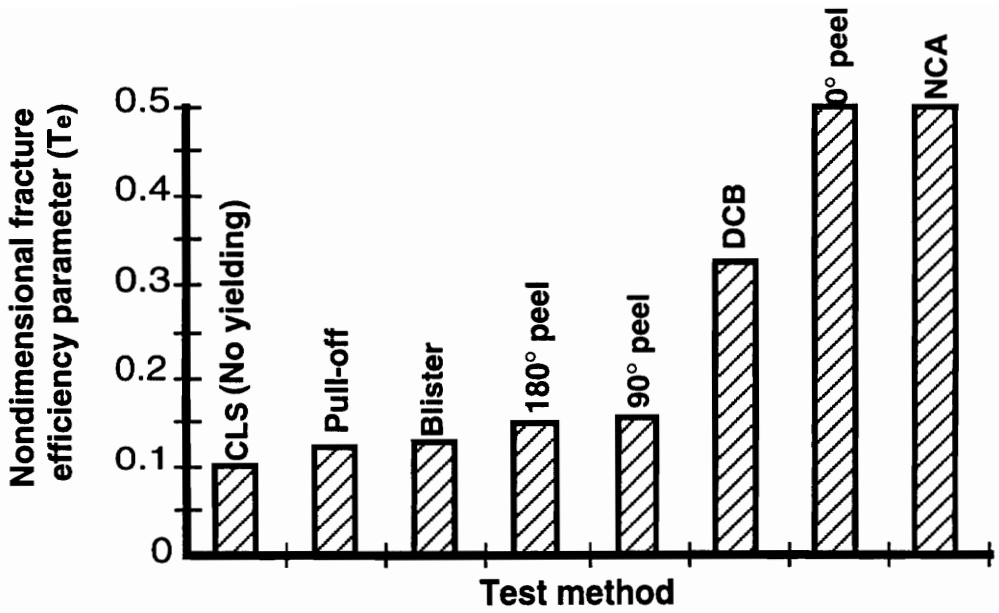

Figure 9. Nondimensional fracture efficiency parameter (T_e) for various types of tests.

Lai and Dillard[37] also introduced a new parameter called the critical fracture efficiency parameter (T_e^c). This is the ratio between the bond fracture strength and the square of the coating strength.

$$T_e^c = \frac{G_C}{\sigma_{cr}^2}, \tag{10}$$

where σ_{cr} is the critical stress of the coating.

When the ratio of T_e^c to T_e equals unity, the coating is at its critical thickness. If the coating is any thinner that this critical value, it will deform plastically. For the NCA test, the critical coating thickness is:

$$h_c = \frac{2G_C\hat{E}}{\sigma_y^2} \tag{11}$$

where σ_y is the yield stress of the coating, and it can be a function of relative humidity if the NCA specimens were intended for durability studies. Equation (11) can be used to check for plastic deformation of the coating and can also be used to design the thickness of the coating.

3.3.2 Finite Element Analysis

ABAQUS software[38] was used to conduct finite element work. ABAQUS is commonly regarded as a powerful finite element tool that processes singularities well[39]. Since the NCA specimen is a fracture test, singularity analysis is very important. A sample code can be found in Appendix A. All elements used were CPE8R. They were two dimensional, eight node, plane strain elements. Since the mesh was simple, reduced integration was used. Only half of the specimen was modeled since the NCA specimen is symmetric with the coating cut as the axis of symmetry. The length of this half model was 40 mm; substrate thickness was 2 mm, and

coating thickness was 0.15 mm. The crack length varied from 0 to 10 mm. Figure 10 illustrates the specimen modeled and its boundary conditions. During the test, a displacement **D** (Fig. 10) is applied to the substrate along its length of it. Figure 11 shows the NCA specimen with an initial debond of 5 mm and a strain of 0.025. Figure 12 shows the mesh around the crack tip when the coating is at the verge of debond propagation. The elements around the crack tip were singular elements. The thicker lines in the figure are the three J-integral contours around the crack tip. Since the results from the third contour were never over one percent apart from the second contour, the third contour results were assumed to be accurate, and all results reported here were from the third contour. The substrate was modeled as an elastic-plastic material, and the coating adhesive as an elastic material.

A model rubber toughened epoxy/steel system was used to compare the analytical solutions to the finite element ones The epoxy modulus was 2.97 GPa and Poisson's ratio was 0.4. The steel had a modulus of 203 GPa, Poisson's ratio of 0.3 and a yield stress of 200 MPa. The thickness of the coating and the substrate was 0.15 and 2 mm, respectively. For this system, Dundurs' parameter α was -0.9. Figure 13 shows G_c plotted against applied strain for both analytical and finite element solutions. There is a very good agreement especially at lower strain levels. Such agreement suggests that solutions for both methods are accurate.

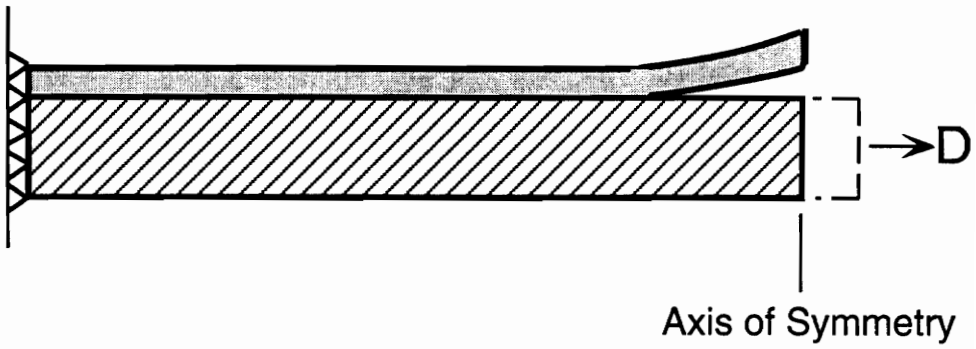

Figure 10. Finite element model of the NCA specimen.

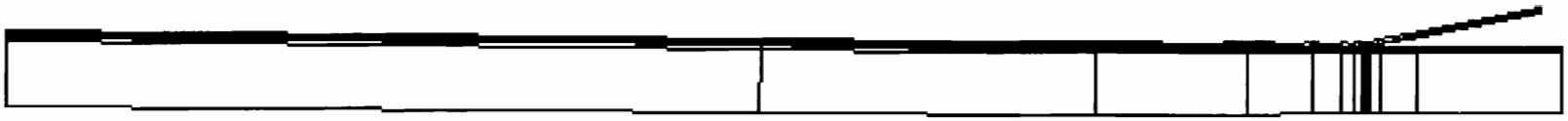

Figure 11. The NCA model when loaded at a $\varepsilon = 0.025$.
(Displacement maginification factor is 4.4)

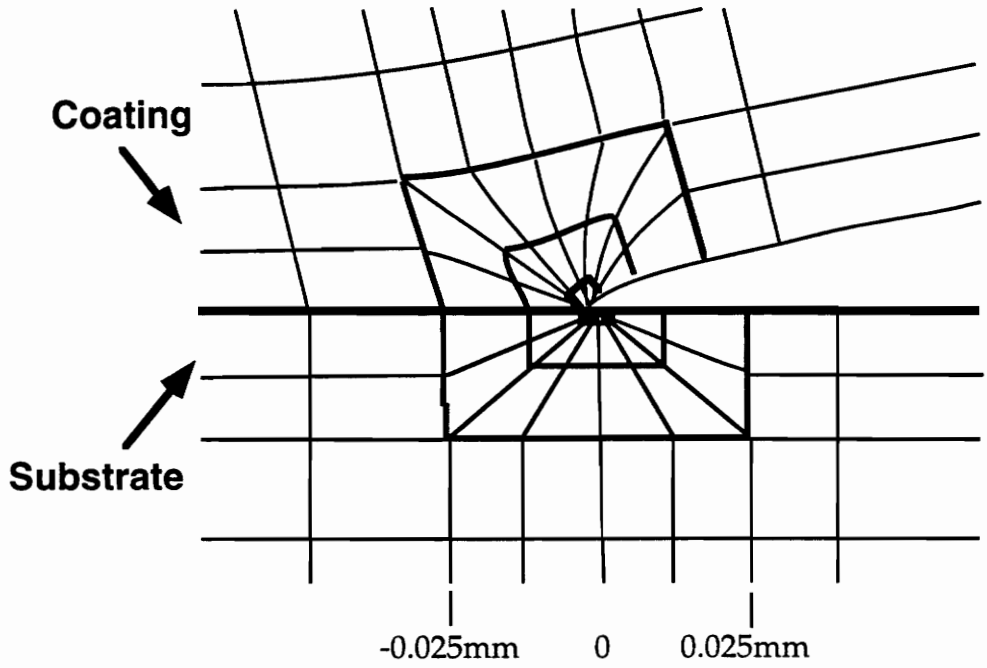

Figure 12. Finite element mesh around the crack tip. (Displacement magnification factor is 4.4).

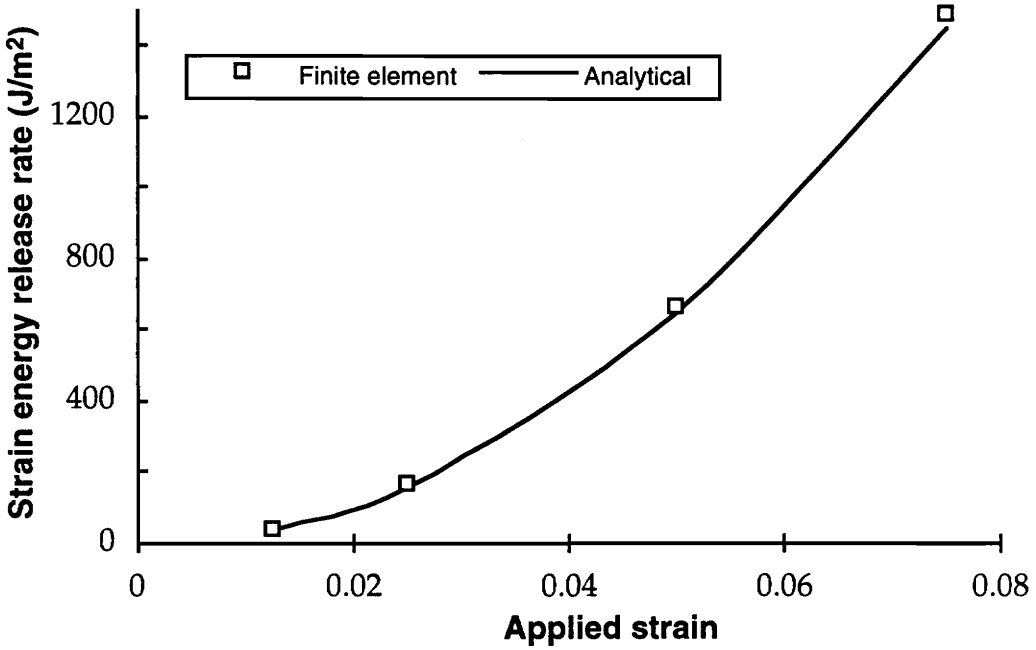

Figure 13. Strain energy release rate versus applied strain for both finite element and analytical solutions. Dundurs' parameter α is -0.9.

In order to verify the validity of both analytical and finite element solutions for different types of systems, analysis were conducted for material systems with various values of Dundurs' parameter α (Fig. 14). The NCA geometric dimensions remained the same. A majority of polymer coated metals have α close to -1. Meanwhile, some polymer coated polymers such as polypropylene coated to low density polyethylene have α of around 0, and for higher positive values of α, we can find systems with metal coated to polymer such as aluminum coated polypropylene for food packaging purposes. For the two extremes of the α spectrum, the two methods of analysis agree very well. For material systems that have α close to zero, there is about 16 percent discrepancy between the two methods of analysis. It is believed that the correction factor for the analytical solution does not work well when α is close to zero.

Finite element analysis was used to determine the effect of initial debond length on **G**. As mentioned before, analytically, the change of **G** at different initial debond lengths is represented by the change of the driving force **Z**. At steady state, (e.g. for long debonds) **G** is constant and Z is 0.5. Figure 15a. shows the effect of the initial debond on the **G** for α = -0.9. Note that **G** approaches steady state at **a/h** = 5 as was mentioned in the previous section. The importance of the analysis is that **G** does not drop significantly as **a/h** decreases. At **a/h** = 1, **G** is less than 2 percent below the steady state **G**. This implies that the initial debond length should not be an important factor for the polymer coated metal systems. Figure 15b is an illustration of the variation of **G** as a function of the initial debond for a positive α (α = 0.9). As the figure illustrates, **G** goes up as **a** becomes shorter. This means that as long as there is an initial cut to the specimen, the initial debond rapidly propagates

to the steady state when tested. Therefore, crack length generated in the initial debond is not believed to significantly affect the results.

Analytically it has been shown that for stiff and/or thick substrates, yielding does not affect the predicted **G** values significantly. Finite element analysis is an excellent tool to study this topic because the properties of the substrate can be easily changed, and results readily obtained. The same epoxy/steel system described above loaded to a strain of 0.025 was used as a model, the steel had a modulus of 203 GPa; however, ε_y was allowed to vary from 0.0015 to 0.025. The two dimensional plane strain model showed that the plastic deformation in the substrate had almost no effect on the results throughout the whole range of yield strain of the steel (Fig. 16). NCA experiments were conducted to study plastic deformation and are described in Section 5.0.

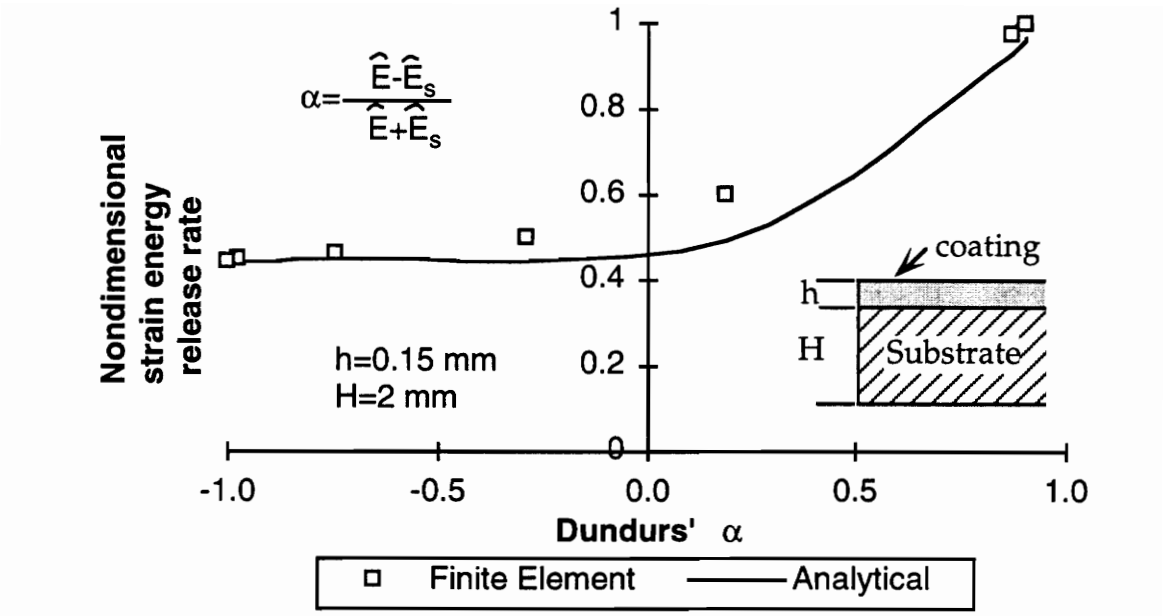

Figure 14. Nondimensional applied strain energy release rate (**G**) versus the Dundurs' parameter α for both finite element and analytical solutions. (To obtain nondimensionality, all values were divided by the highest value obtained)

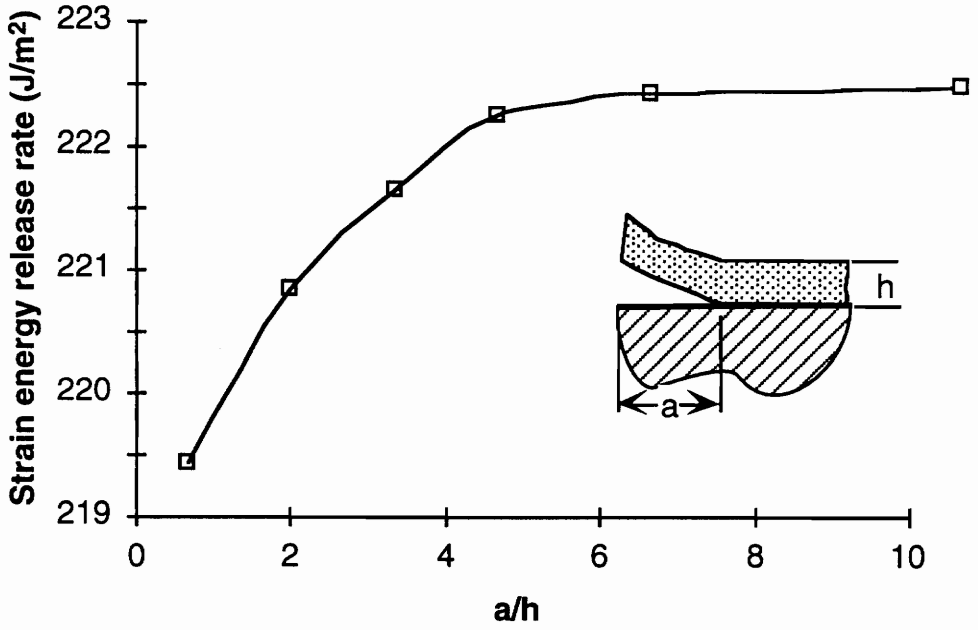

Figure 15a. Applied strain energy release rate (G) versus nondimensional initial debond length for the case of Dundurs' α = -0.9.

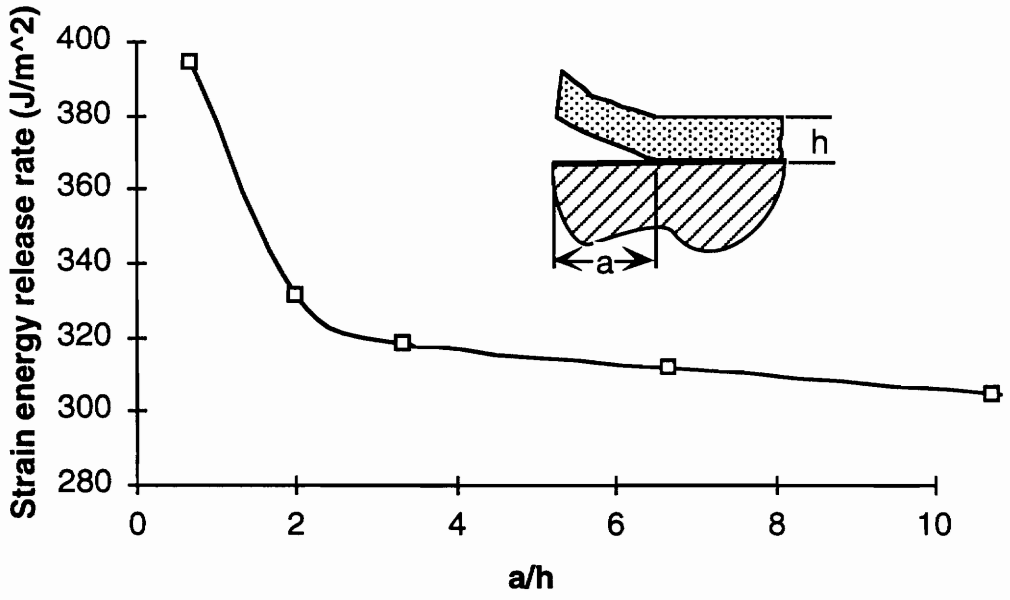

Figure 15b. Applied strain energy release rate (G) versus nondimensional initial debond length for the case of Dundurs' α = 0.9.

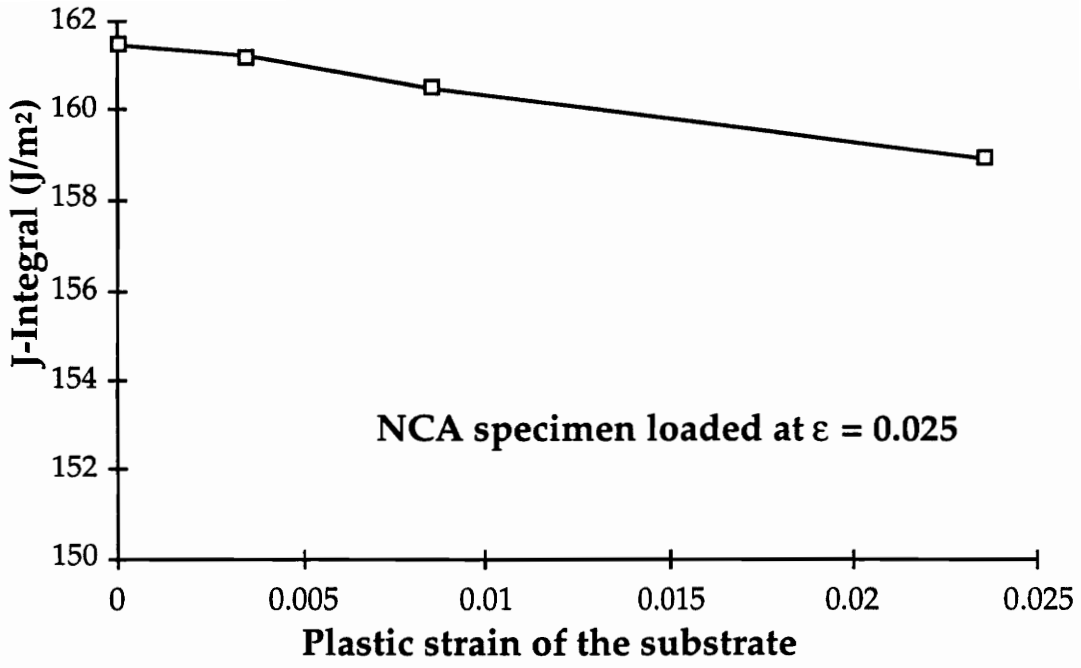

Figure 16. J-Integral versus the plastic strain of the substrate

3.4 Limitations and Possible Solutions

Since this thesis is based on discussions about the NCA test, one important study is naturally on the limitations of the test. If one chooses to avoid large plastic deformation on the substrate or plastic deformation on the coating, one has to increase the thickness of the coating. If we assume the residual stresses, G_C, ν and the moduli to be constant and the modulus of the substrate is much higher than the modulus of the coating, equation (4) can be simplified to:

$$\frac{1}{h} \propto \varepsilon_C^{\,2} \tag{11}$$

Where ε_C is the critical strain. One can see from Eq. (11) that by increasing the thickness of the coating, the strain required to generate the same applied **G** decreases; therefore, reducing and eventually eliminating plastic deformation of the substrate and/or the coating.

A limitation to the NCA test is that during the test neither the coating nor the substrate can break, or have internal cracks before debond occurs. If the maximum strength for both the substrate and the adhesive are known, then Eq. (11) can also be used to determine the correct thickness of the coating that will generate debond propagation before either material fails. Note that since the substrate thickness usually has very little effect on the determination of **G**, its thickness effect is normally ignored.

Another restriction is that the test does not work well with soft coatings such as elastomers. Because of their low modulus, these adhesives tend to elongate with the substrate without debonding. There are however, two solutions to the problem. The first solution is to add a backing to the adhesive (Fig. 17a). The backing adds stiffness to the adhesive and aids in causing debond at lower strains. Care must be made in choosing the correct

backing. It must be tough enough that it will not crack prior to coating debonding. Since there are now two interfaces, the bond between the coating and the backing must be stronger than the bond between the coating and the substrate to ensure that debonding occurs along the right interphase. Successful experiments that utilize this approach include the pressure sensitive adhesive on Kapton and 3M's Scotch tape backing bonded to various substrates. If the specimen is intended for durability studies, care must be made to ensure that the backing is permeable to solvents or the backing can be added after specimen conditioning and before testing. If the second option is chosen, the time taken to cure the backing and the curing method should not cause any significant changes to the saturation conditions to the first interphase.

The second possible solution to solve the problem of the coating being too soft is to embed a scrim cloth into the coating (Fig. 17b). The addition of the right scrim cloth may increase the modulus of the coating (adhesive plus cloth) to the required level for the NCA test. In case the specimen is intended for durability studies, scrim cloth is used so that solvents are free to pass through it into the interphase, yet provide the needed stiffness. When scrim cloth is used, there is no need to worry about the bond strength between the adhesive and the cloth, but for certain adhesives, it may not be practical to insert scrim cloths.

Table (1) adapted from Evans *et. al.* illustrates the possible problems caused by substrate/coating properties on modes of NCA decohesion[40]. Note that the debond mechanisms described occur only at extreme situations.

During specimen fabrication and preparation the researcher must exert care on some features. The specimens should have uniform coating thickness especially near the initial debonded area. If non-uniform thickness

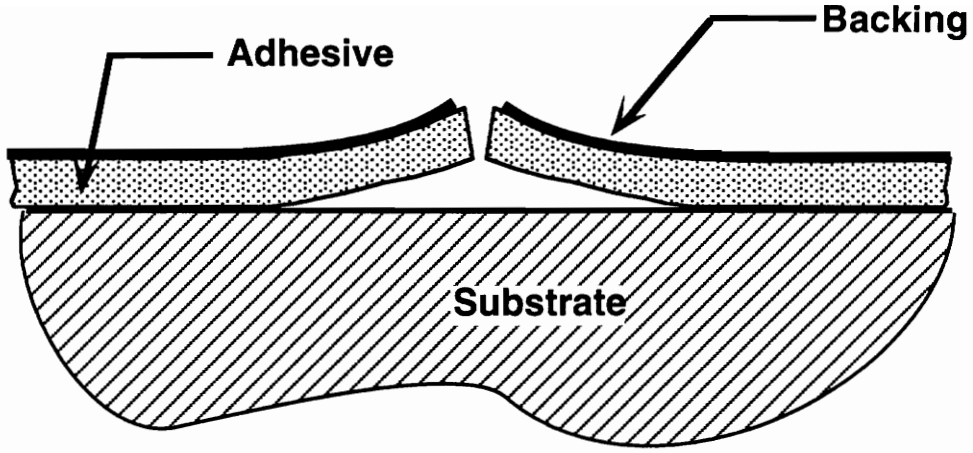

Figure 17a. Adhesive coating with a backing attached.

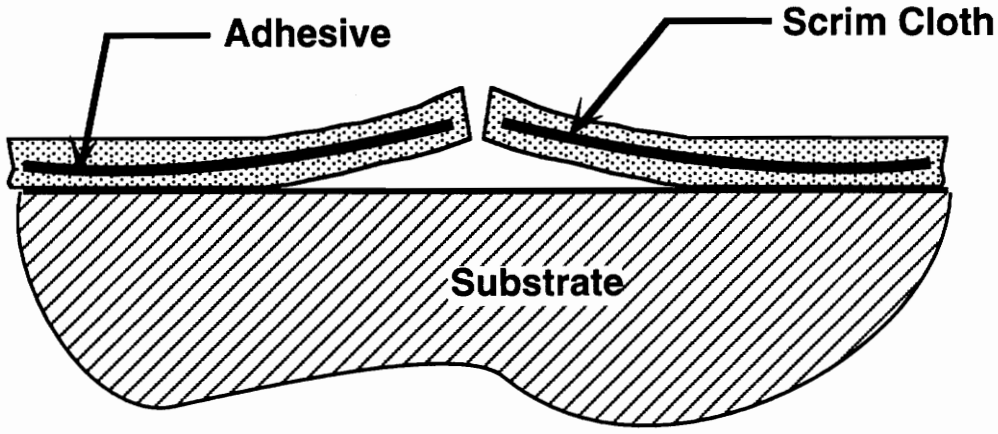

Figure 17b. Adhesive with a scrim cloth embedded.

exists in this region, the debond propagation might deviate from the self-similar assumption. The crack front tends to move faster in the thicker region and slower in the thinner region causing the debond to propagate in an unstable manner making the propagation difficult to detect and to quantify. Chipped adhesive and rough edges near the initial crack area should be avoided since these factors may affect the driving force **Z**.

The advantage of having a short diffusion path may also be disadvantageous in some situations. If the NCA test is to be used to determine the bond strength without environmental effects, specimens must be tested immediately after fabrication or they must be placed in a desiccater. If not, the interphase may be saturated at room humidity conditions. If however, a durability studies is being carried out, the specimens can be placed in the conditioning chamber for longer periods of time without problems.

Probably the most important shortcoming of the NCA test is that since the specimen failure is interfacial and all built in stresses are released when the debond propagates, these stresses and properties of the coating must be accurately known. The stresses include residual stresses due to curing and stresses caused by moisture or solvent ingression. The modulus of the coating must be known and in the case of moisture or solvent ingression studies, the modulus should be that of the conditioned coating. Unfortunately, little relevant data on engineered polymers exists, so actual experiments to determine these properties may be required. The stresses and the modulus are not always easy to determine. Many times, experiments must be conducted to determine the coefficient of thermal expansion and swelling due to moisture for both the substrate and the coating in order to estimate residual stress and stress due to moisture respectively. For determining modulus, tests such as stress-strain tests should be conducted. In the case of durability studies, modulus tests must be conducted with the

sample saturated with the introduced solvents. For the systems studied in this research, residual stresses contributed from 0 to as much as 50% of total **G** depending on the system. Therefore, to accurately determine debond toughness with NCA an accurate knowledge of residual stresses may be important. In case the NCA tests are being conducted as a comparative tool to study similar systems, such as surface treatment studies with the same coating and substrate, the stresses might not be needed since they will probably be the same. The modulus of the coating in this case also does not need to be accurately determined for the same reason.

Table 1. Possible modes of NCA decohesion. (Adapted from Evans, et. al.[40])

Coating	Substrate	Interface bonding	Debond mechanism
Brittle	Ductile	Good	Coating cracking, no debond
Brittle	Ductile	Poor	Film cracking, with debond
Ductile	Brittle	Good	Edge decohesion in substrate
Ductile	Brittle	Poor	Edge decohesion at interface
Ductile	Ductile	Good	Coating/substrate splitting
Ductile	Ductile	Poor	Edge decohesion at interface
Brittle	Brittle	Good	Buckle propagation in adhesive
Brittle	Brittle	Poor	Coating cracking, edge decohesion at interface

4.0 DURABILITY STUDIES

One of the main reasons that adhesives are not more widely used for structural applications is the difficulty in predicting long-term durability. For example, adhesive joints exposed to humid environments typically lose some of their strength. Therefore, a system that exhibits high initial strength in laboratory tests may fail unexpectedly at much lower loads when exposed to humid environments over time. Many adhesively bonded structures are expected to encounter humid environments, necessitating a thorough understanding of the effects of moisture on adhesive systems. As stated in the Background (Section 2.0), a majority of currently used tests for durability studies are costly or yield only qualitative data.

The development of the NCA test began with the objective of being able to accurately and rapidly determine environmental effects on adhesive systems. Therefore, it is only natural to have detailed studies on NCA's performance in determining adhesive system's durability. Both NCA and DCB tests were used to study the durability of steel/epoxy systems so that the results could be compared. Accelerated durability studies using DCB specimens are usually accepted as a good research practice, and it is a widely studied test. Hence, it is chosen as the control test.

4.1 Adhesive Systems

For all experimental procedures described in this section, cold-rolled 1018 steel was used as the substrate. The adhesive studied was a model Dow Chemical epoxy system designed for potential automotive applications. The formulation for this adhesive is shown in Table 2. The formulation corresponds to the formulation in Rakestraw et. al.'s paper[41]. The epoxies

used were Dow Chemical D.E.R. 331, a low molecular weight bisphenol A-type resin, and Reichhold Chemicals KELPOXY G272-100, an epoxy terminated elastomeric copolymer containing approximately 40% rubber. The epoxy was cured using dicyandiamide (DICY) as a curing agent and 3-phenyl-1,1 dimethyl urea (PDMU) as a curing accelerator. This epoxy contains approximately 8% rubber. To prepare the adhesive, the epoxy resin D.E.R. 331, DICY and PDMU were placed in a 1 gallon Ross mixing pot. The epoxy resin was mixed at a speed of approximately 18 r.p.m. until the DICY and PDMU were homogeneously mixed into the resin and no powder was visible. The speed was increased to about 72 r.p.m. and a vacuum was employed to about 28 inches of mercury. After 15 minutes, fumed silica was added as filler. After the silica was "wet," the mixer was started at 18 r.p.m. and slowly increased to 72 r.p.m. and then 100 r.p.m. With the vacuum on, mixing was continued for 15 minutes. Kelpoxy was then added and mixed with the resin for 5 minutes or until all visible air bubbles were removed. At this point, mixing was stopped, and atmospheric pressure was slowly reintroduced back to the mixing pot. All specimens were cured at a temperature of 155°C for 90 minutes. For all experimental procedures described in this section, the steel was polished with a 600 grit sand paper, and wiped with generous amounts of acetone.

4.2 Set Up for Humidity Conditioning of Adhesive Systems

For humidity studies, it was decided that specimens were to be conditioned in humidity chambers under several different humidity levels while maintaining a constant temperature of 60°C. The constant temperature was chosen to simplify the test matrix and concentrate the efforts solely on

Table 2. Formulation for the Dow Chemical model epoxy

Adhesive Component	Name	Description	Percent Weight
epoxy resin	D.E.R. 331	liquid bisphenol A-type resin	69.1
curing agent	dicyandiamide (DICY)	solid latent curing agent	4.1
curing accelerator	3-phenyl-1, 1 diethyl urea (PDMU)	tertiary amine accelerator for dicy-cured epoxies	1.6
filler	M-5 silica	hydrophilic fumed silica	4.9
rubber-toughener	Kelpoxy G272-100	epoxy terminated copolymer	20.3

the humidity effects. While 60°C seemed high enough for water to diffuse at a reasonably fast rate without degrading the polymer structure, more studies still need to be conducted to investigate this assumption. A simple DSC test should suffice in comparing the physical properties of adhesives that were exposed to moisture in room temperature and at 60°C.

Several water baths were set up to condition specimens at different humidity levels. The edges of the cover were taped to the chamber with masking tape to make it almost air tight. Specimens were placed on stands so that they did not come in contact with the solution (Fig. 18). Constant relative humidity levels were maintained by means of aqueous glycerin solutions in the water bath. The solutions were prepared according to ASTM standard method D 5032-90[42]. Different concentrations of glycerin solution in distilled water yielded reservoirs that had different humidity levels. Conditioning humidity levels varied from 0 to 94% RH. The humidity levels were constantly monitored with a humidity probe to keep the solution within 2% of the desired relative humidity. Deviations were adjusted by either adding glycerin or water to the water bath.

Several researchers[7,24,43] have noted the existence of a critical relative humidity. Adhesive systems exposed to humidity levels below this critical relative humidity usually do not lose much of their strength. At humidity levels above this critical value however, the strength of the system quickly declines. The critical humidity level is generally thought to be around 70% RH for epoxy based systems.

To learn about the adhesive system's durability, specimens were conditioned at 0, 25, 50, 80 and 94% relative humidity (RH) and at 60°C. 0% RH specimens were used as controls. Specimens conditioned in this environment were not expected to lose any strength. Specimens at 25 and

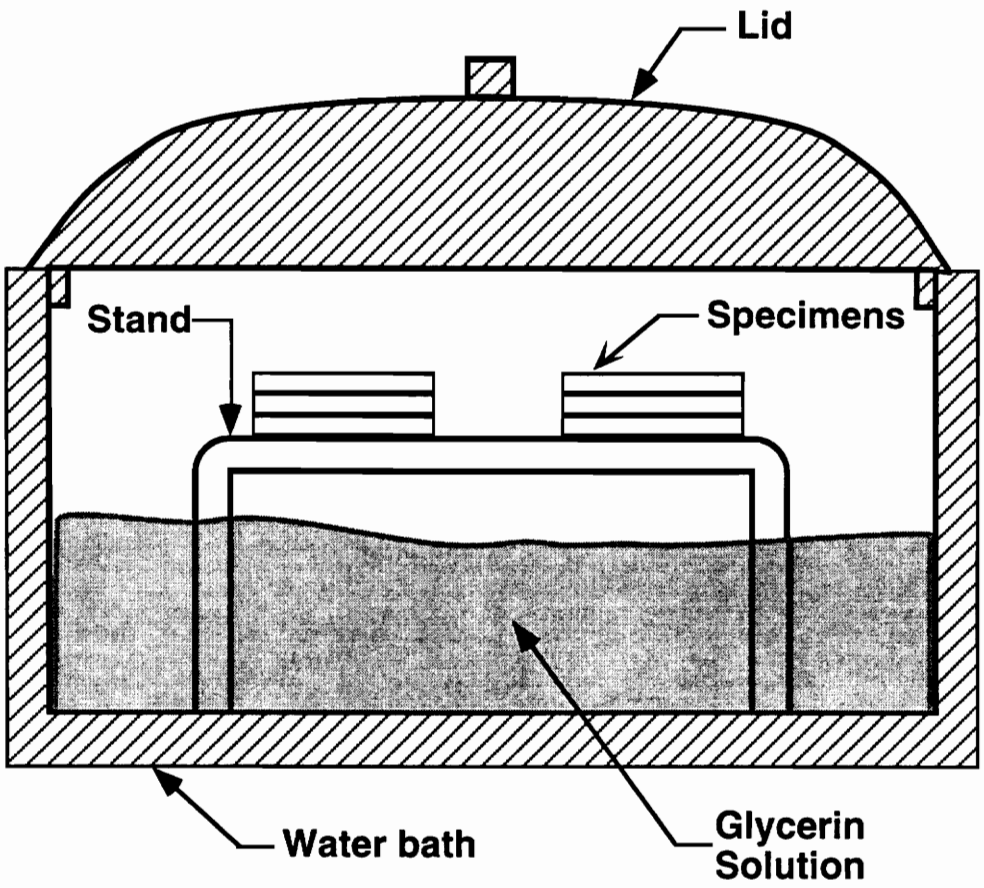

Figure 18. Cross sectional schematic of the conditioning chamber.

50% RH should be on the lower side of the critical RH. Therefore, not much strength should be lost. Specimens conditioned in both 80 and 94% RH were expected to dramatically lose their adhesive characteristics when equilibrium was reached. 94% RH was chosen because it was the value that was close to 100% yet did not cause water condensation on the specimens in the humidity chamber used.

4.3 Moisture Ingression Tests

If water enters an adhesive by diffusion, and if such phenomenon has been determined to be Fickian or quasi-Fickian, then it is possible to estimate the distribution of water using Fickian equations. The objective here was to determine the diffusion rate and saturation profiles of bulk adhesive. This test was also used to determine the exposure times necessary to achieve equilibrium moisture levels for both types of specimens.

Kinetics of moisture ingression tests were conducted on samples of the bulk adhesives for several humidity levels. The rubber toughened epoxy adhesive systems were exposed to several relative humidity levels while maintaining a constant temperature of 60°C. In the past, diffusion in epoxy systems has been shown to be Fickian even at temperatures below Tg[7,23,44]. According to Comyn, the characteristics of the Fickian sorption can be summarized in four points[45]:

1) Sorption curves are initially linear with respect to $t^{0.5}$; this linearity extends to at least $M_t/M_\infty = 0.6$.

2) Above the linear region, curves are concave against the abscissa.

3) Plots of M_t/M_∞ against $t^{0.5}/h$ which are termed reduced sorption curves, should coincide for films of different thickness.

4) Reduced sorption curves will only coincide when diffusion constant does not vary with concentration of the sorbant.

Assuming the specimen is a semi-infinite film so that the diffusion into the edges can be neglected, and one dimensional diffusion model can be used, the diffusion rate can be found by determining the fractional uptake which is expressed as[46]:

$$\frac{M_t}{M_\infty} = 1 - \frac{8}{\pi^2}\sum_{n=0}^{\infty}\frac{1}{(2n+1)^2}\exp\left[\frac{-(2n+1)^2\pi^2 Dt}{4\ell^2}\right] \qquad (12)$$

Where: M_t is the mass of the diluent in the polymer at time t;

M_∞ is the mass of the diluent in the polymer at equilibrium;

D is the diffusion constant;

t is the conditioning time, and

ℓ is the thickness of the sample.

At short times ($\frac{M_t}{M_\infty} < 0.6$), when the fractional uptake is approximately linear with the square root of time, the above expression can be approximated as[46]:

$$\frac{M_t}{M_\infty} = \frac{4}{\ell}\left(\frac{Dt}{\pi}\right)^{\frac{1}{2}} \qquad (13)$$

Once moisture uptake data was obtained, the diffusion constant could be estimated by using the above equation (Eq. 13).

A 2 mm thick unsupported film was considered the ideal thickness for the moisture uptake research on this particular type of epoxy. A 1 mm thick specimen gave inconsistent results probably due to the lack of accuracy at small weights, and it took a long time for 3 mm thick specimens to reach equilibrium (roughly 115 days in water at 20°C)[7]. Some scatter was always inevitable since the specimens have low percent weight gains at equilibrium. Compared to other researchers' results[7,42,47] on specimens that have low weight gains, the data obtained were reasonable. The width and height of the specimen were at least 15 times that of the thickness[47]. This requirement was set so that the diffusion rate can be determined by considering the specimen as a semi-infinite film.

In the past, other researchers have dried specimens by blotting them with paper. After working with different papers and cotton to dry specimens, it was found that cotton worked best. When the specimen was to be measured, a piece of cotton ball was used to lightly rub the surface of the specimen until no water could be seen. The films were measured and then quickly placed back in the conditioning chamber.

Figure 19 shows a typical moisture uptake chart. Moisture was absorbed into the bulk adhesive until equilibrium values of mass uptake were obtained. The results obtained agree with Comyn's last three points on Fickian characteristics. Although the graph did not demonstrate a pure linear relationship before M_t/M_∞ reached 0.6, it was assumed the line was closely linear, and the data was modeled using Fickian kinetics. Ficks law requires that the diffusion constant be independent of moisture content; if there is moisture dependency, it renders the fundamental Fickian equation nonlinear. The data collected showed that diffusion constant is a function of moisture content. Therefore, the epoxy system studied does not behave in a strickly Fickian manner. Despite being moisture dependent, diffusion

constants for each humidity level were estimated with the Fickian one dimensional model.

The diffusion constants at various conditions calculated using equation (13) are listed in Table 3. The numbers are averages of three samples. The diffusion constants and water concentration increased as the conditioning humidity levels increased. Diffusion in water appeared to be slower than diffusion in 98% RH, perhaps because low molecular weight materials in the adhesive might have leached out of specimens when submerged in water. The maximum water concentration was unusually high compared to the data found in the literature[7]; however, it is not unique, some researchers also found relatively high water concentration levels in epoxy systems (*e.g.*, Comyn *et. al.*[24]).

The results show the diffusion constant's dependency on the relative humidity levels which suggests a non-Fickian behavior. However, with the diffusion constants estimated, it is possible to estimate the required time to condition specimens to saturation at each humidity level using Eq. (13). Since 50% RH had the lowest diffusion constant, to be on the conservative side, it was decided to use this value to estimate conditioning times for all specimens. For a 0.5 mm thick NCA, the diffusion path is the thickness itself, and the time to saturate the specimen was estimated to be 40 hours at 50% RH. Since this is only an estimate, it was decided to condition specimens for at least 3 days. This duration should be long enough to have all specimens saturated. Although the diffusion constant for 25% RH was not determined, but it was used for NCA tests, it is believed that the three day period is conservative enough for the 25% RH condition. For a 12.7 mm wide DCB, the diffusion path is 6.35 mm, thus, the diffusion time is 270 days. The conditioning time for DCB's ranged from 336 to 360 days. Water diffusion in

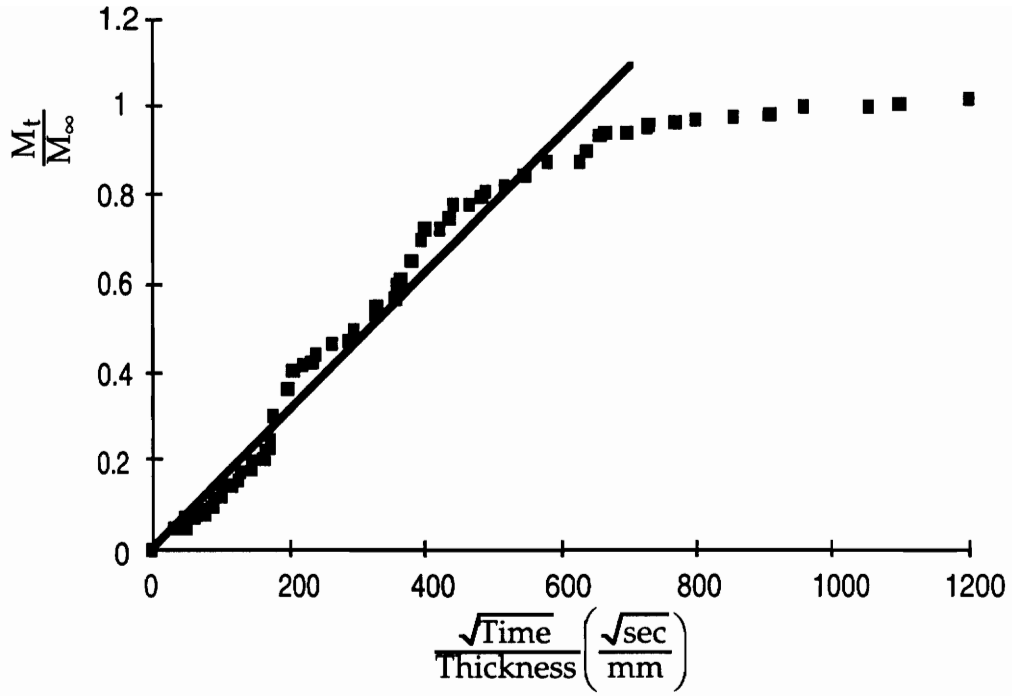

Figure 19. A mass uptake chart for rubber toughened epoxy adhesive. Temperature is 60°C, and relative humidity is 98%. The line is the diffusion constant line.

Table 3. Diffusion constants for epoxy adhesive at various conditions.

Condition	$Dx10^{-7}\frac{mm^2}{sec}$	C_∞
20°C, water	2.44	1.97%
60°C, water	5.08	2.7%
60°C, 98%RH	6.28	4.5%
60°C, 75%RH	5.90	2.47%
60°C, 50%RH	3.36	1.75%

C_∞ is the water concentration in the sample at equilibrium.

a DCB specimen might be somewhat faster than in bulk because water might wick through the specimens from the interphase, and it probably had time to react with the substrate and the interphase as the water diffuses . Therefore, it was assumed that conditioning in excess of 300 days was adequate. After the tests, the interphase was visually inspected, and all conditioned DCB specimens appeared to have saturated adhesives because the interfaces of all failed specimens were wet and the entire steel surface showed signs of corrosion. Since DCB specimens were conditioned for a long period of time, they were periodically inspected, and the accumulated rust was periodically removed.

4.4 Determining Stresses In The Bond

Because when a coating debonds, all stresses in the debond region are released, it is necessary to recognize the various stresses present in the bond. These stresses are generated by adhesive swelling due to moisture, and thermal residual stress. To determine these stresses it is necessary to find out the amount of linear swelling due to moisture, the coefficient of thermal expansion and the modulus of the saturated adhesive.

A Polymer Laboratories' Miniature Materials Tester (Minimat) was used to determine the modulus of saturated adhesives. The specimens were fabricated by casting a 1 mm epoxy film with a casting blade and curing at 150°C for 90 minutes. The samples were then cut into rectangles of 30 mm by 5 mm. The specimens were conditioned at appropriate humidity levels at a temperature of 60°C for 3 days and then tested. The crosshead speed was 0.1 mm/min., and the gage length was approximately 15 mm. The load (**P**) and the strain (ε) were recorded, and the modulus was determined by finding the

linear range of the slope of **P** over ε and dividing that by the cross sectional area.

Plotting load versus change in displacement of the crosshead is normally considered to be an inaccurate method to measure modulus. Probably the most commonly accepted method to measure modulus is to determine the slope of load over strain measured by extensometers and strain gages. In the case of this durability studies, strain gages were not a good option because, during the period required to install strain gages, considerable water might have evaporated from the specimens. On the other hand, if an extensometer was used, it had to be firmly attached to the specimen; this required specimens to be stiff. For the epoxy system used, the appropriate thickness for the use of an extensometer was found to be 3 mm thick. In durability studies, 3 mm thickness means that a long conditioning time is required. In contemplating the possibility of using Minimat to determine modulus, a comparison test was conducted between the Minimat test and the standard tensile test with large dogbone specimens and an extensometer on unconditioned adhesives. After comparing three tests, the average result obtained from the Minimat test was only six percent smaller than the one determined using an extensometer. Assuming that six percent error was acceptable, and that it was important to save time in conditioning the specimens, it was decided that the Minimat test was to be used to obtain modulus values for the conditioned samples.

Specimens of dimensions 40 x 3 x 0.15 mm were prepared. Three replicas were tested for each humidity level. These specimens were placed in humidity chambers until they became saturated. The specimens were then taken out of the chambers, left to cool down to room temperature and tested. The modulus as a function of saturated moisture is plotted in figure 20.

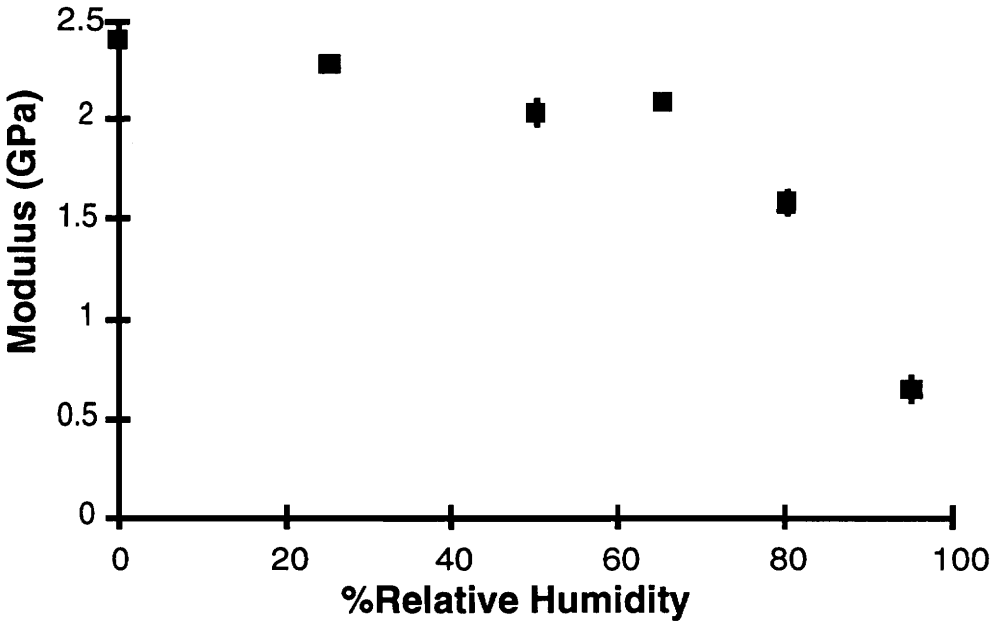

Figure 20. Adhesive modulus as a function of conditioning percent relative humidity. (The error bars are ± one standard error from the mean)

Linear swelling tests of the bulk adhesive were conducted. Data obtained here were used to determine stresses caused by moisture ingression. Swelling data was collected on the same specimens as the ones used for moisture uptake tests. Before specimens were conditioned, two points were marked on the adhesive film with a razor blade at two locations distant from each other (≈30 mm). The distance between these two points was measured using an optical microscope equipped with cross hairs. After the moisture uptake reached equilibrium, the specimens were taken out of the chamber, left outside for sometime to cool down to room temperature so that thermal expansion is eliminated. Then, the distance between the two marked points was measured again. The difference in the distance readings was assumed to be caused by moisture-induced swelling. Figure 21 shows the swelling data. This information can then be used to determine stresses due to moisture swelling in an adhesive system. Since the data has a linear relationship, a simple equation can be written:

$$\text{(Linear Swelling)} = 8.4 \times 10^{5} \text{ (\% Relative Humidity)} \qquad (14)$$

Since steel is non porous, it is assumed that moisture causes no physical changes to steel. The stress due to moisture is then solely caused by the coating's deformation. This stress can be found with the following expression:

$$\sigma_m = -(8.4 \times 10^{5})(\text{\% Relative Humidity})(E) \qquad (15)$$

Where E is the modulus of the adhesive after humidity conditioning.

Small adhesive samples, approximately 5 x 5 x 3 mm, were cut using a diamond saw, and the surfaces were polished with silicon carbide grinding paper. The specimens were placed in a TA Instruments 943 thermal mechanical analyzer (TMA) to determine the coefficient of thermal

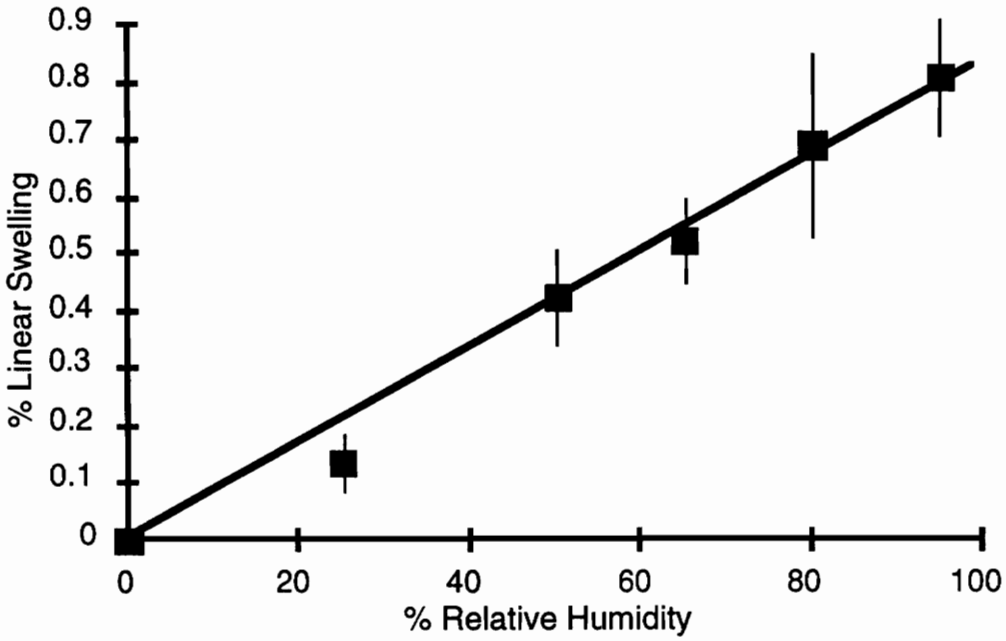

Figure 21. Linear increase of the swelling of the adhesive film. (The error bars are ± one standard error from the mean. The line is a linear regression from all data points.)

expansion (CTE). For temperatures below glass transition temperature (Tg), the CTE was found to be 68 x 10^{-6}/°C. Since steel is on the order of 70 times stiffer than the adhesive, it was assumed that steel does not deform and that polymers are free to flow above Tg. The thermal residual stress can be estimated:

$$\sigma_t=(CTE)(Tg-T)(E) \qquad (16)$$

Where E is the modulus of the adhesive after humidity conditioning.

4.5 Notched Coating Adhesion Test Results

Two Teflon coated steel slabs were used to sandwich NCA specimens during fabrication. These slabs were used to generate a uniform thickness to the specimens and to keep them from bonding to any undesired surfaces. Nine steel strips were placed on one slab in addition to five surrounding strips that served as the dam. A small space was left on either side of the dam to allow extra adhesive to escape. 0.3 mm thick Teflon Strips were taped on the dam strips to generate 0.3 mm thick coatings. After wiping the steel strips with generous amounts of acetone, the adhesive was poured and spread over the strips. The specimens were covered with the second slab and placed in a programmable hot press. They were cured at 155°C for 90 minutes. Six specimens were fabricated for each humidity condition tested. After removal from the hot press the specimens were immediately placed in humidity chambers.

After the specimens were properly conditioned, precracks were introduced and specimens were tested as described in Section 4.0. The specimens were tested at a crosshead speed of 1 mm/min. in an Instron screw driven universal loading frame. A LabVIEW data acquisition system was used to collect strain information from an extensometer attached to the

substrate side. Crack movement was observed visually and the critical strain at which the debond propagated was recorded. Strain energy release rate as a function of modulus was determined and plotted in figure 22. Statistics analysis showed that for the significance level (alpha) of 0.05, each relative humidity level tested generated a significantly different G_C. In another words, change in humidity levels, even in smaller increments, is a determinant in the strength of the adhesive bond.

To determine the mode contributions to the SERR, Dundurs' parameters α and β were determined. They are -0.97 and 0.16 respectively for the material system used herein. From the Dundurs' parameters, it was found that: $G_{II}/G_I = 1.7$.

4.6 Double Cantilever Beam Tests

As previously mentioned, double cantilever beam (DCB) (Fig. 23) tests were chosen as the comparison test for the durability research. For static DCB tests, the arrest, critical and maximum strain energy release rates and the fracture type can be identified, but this paper is only concerned with the critical values. For a more detailed treatment on DCB properties and analysis, refer to Rakestraw et. al.'s paper[41]. Note that in this paper, G_C and G_{arrest} are considered to be the same.

4.6.1 Specimen Fabrication

Due to the quantity of specimens required for the durability studies, specimens were made by first bonding 0.25" x 9" x 14" panels of 1018 steel and then cutting individual specimens from these panels using a waterjet cutting machine. After applying an acetone wipe on one steel panel, Teflon tabs and

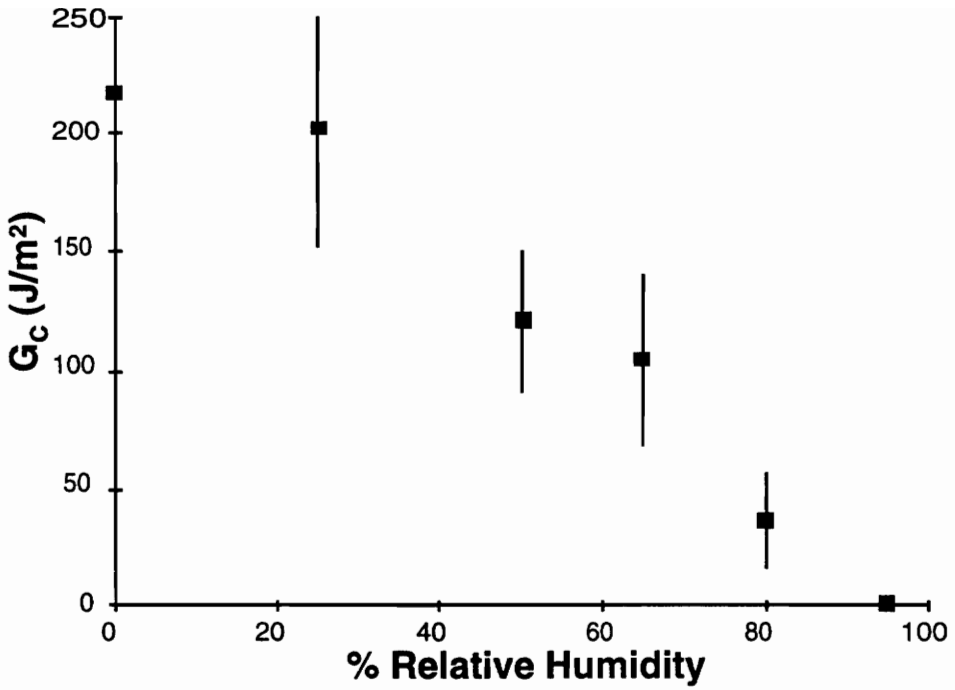

Figure 22. G_C versus percent relative humidity determined from NCA tests. (The error bars are ± one standard error from the mean.)

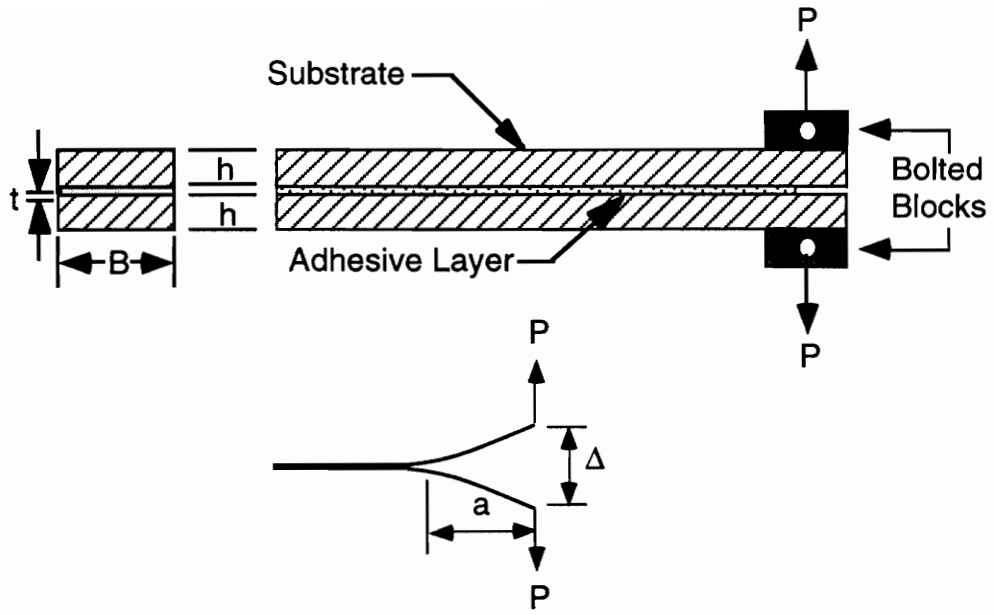

Figure 23. The double cantilever beam specimen and a schematic diagram of the deformed specimen.

appropriate sized wire strips (to control bond thickness) were taped onto it. Kapton tape was used to hold the Teflon and the wire in place. After the cure process was complete, Teflon tabs were removed; this helped to produce the sharp starter crack. The adhesive was then poured onto the surface of the steel and smoothed to the desired thickness (0.8 mm) with a Teflon spatula. Finally, the second adherend was placed on top of the steel plate containing the Teflon, wire, and adhesive. The resulting specimen was bonded in a programmable hot press and cured at a temperature of 155°C and a pressure of 33 KPa for 90 minutes. The specimens were then waterjet cut, drilled, tapped, polished and placed in humidity chambers for conditioning.

Since the objective was to determine the effects of humidity on the durability of the adhesive system, and since diffusion of water into the DCB adhesive takes a long period of time, the ASTM standard 1" wide DCB specimen was no longer practical. According to calculations, such a specimen would take about 1200 days to reach equilibrium at 60°C. It was therefore decided that the majority of the new DCB specimen would be 1/2" wide. This reduced the time to reach equilibrium to approximately 270 days. Some 1" wide DCB's were made to investigate whether the width difference played any role in strain energy release rates obtained.

4.6.2 Static Analysis

Static DCB specimens were tested in an Instron machine controlled through its GPIB interface using LabVIEW software. The specimens were loaded at a crosshead speed of 1 mm/minute. As the specimen was loaded, a hand held microscope and the load-deflection curve (which appear on the LabVIEW program used to control the test) were used to detect critical events taking place in the specimen. For example, when the curve deviates from

linearity (Point A on Figure 24), the crack had begun to grow. This observation was visually confirmed by the hand held microscope. Now, due to the rate dependent interfacial failure of these adhesive systems, the loading value continued to increase until the load reached a maximum and began to rapidly decrease (Point B on Figure 24).

Once the maximum loading was detected, the crosshead motion was stopped to allow the crack growth to continue until it reached near-equilibrium conditions (Point C on Figure 24). The term near-equilibrium is used because the crack was not always allowed to *completely* stop. The criterion used to establish a reasonable critical loading level was that the strain energy release rate decreased by less than 1 J/m^2 per minute. This procedure was used to identify the critical fracture energy, $\mathbf{G_{Ic}}$. The vertical lines on Figure 24 resulted from the crack growing while the crosshead position was being held constant. Once crack growth slowed sufficiently, the specimen was unloaded to make sure plastic deformation of the adherends had not occurred. If plastic deformation had occurred, the **P-Δ** curve will not return to the origin, but instead will intersect the deflection-axis to the right of the origin. Finally, this load-hold-unload procedure was repeated until the specimen was fully fractured.

The compliance-beam method was used to analyze the data. Since DCB specimen fails in mode I, the strain energy release rate (G_I) becomes:

$$G_I = \frac{P^2(a+x)^2}{B(EI)_{eff}} \tag{17}$$

Where: $(EI)_{eff}$ is the effective flexural rigidity of the DCB specimen as defined by the experimental data;

I is the moment of inertia of the adherends;

B is the specimen width;

a is the crack length, and

x is the apparent crack length offset as defined by the experimental data.

For a more detailed treatment please refer to Rakestraw *et. Al.*[41].

4.5.3 Results

DCB specimens were conditioned for at least 336 days. At least two specimens were tested for each humidity condition; each specimen yielded from three to five G_{Ic} values. The averaged results are plotted in figure 25. The results show the same adhesion strength dependency on relative humidity levels as the NCA tests have shown.

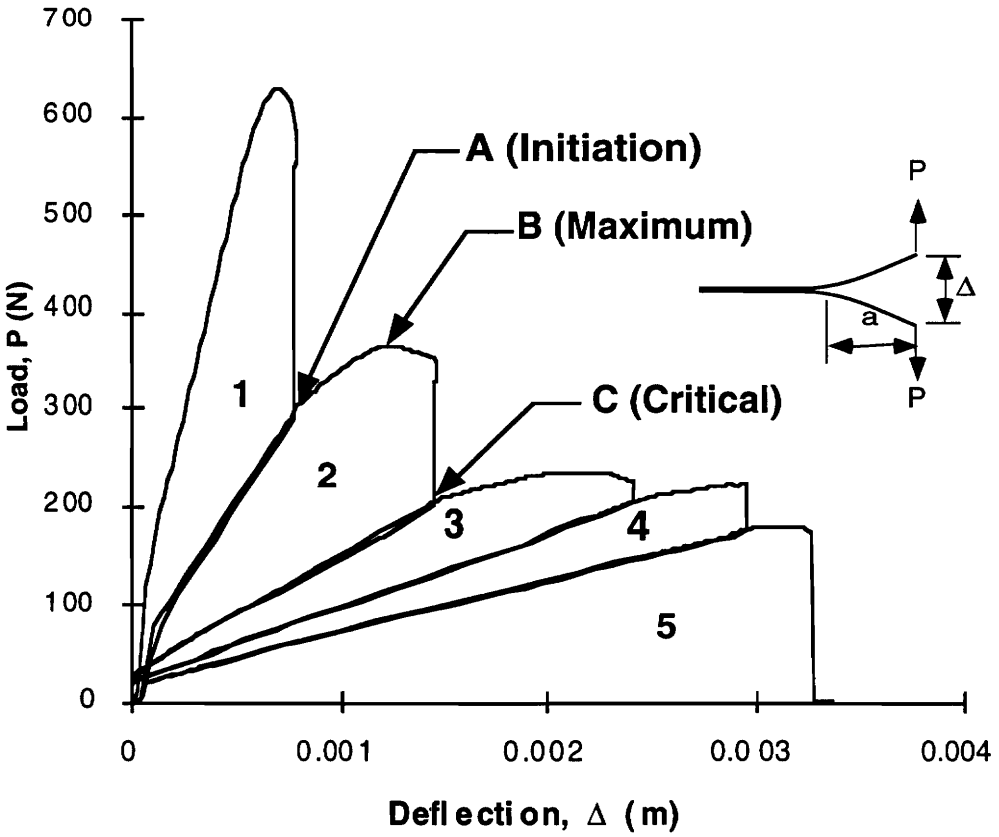

Figure 24. A typical load-deflection curve from a quasi-static DCB test showing 5 load-unload cycles and critical points on the curve. Data is from sample 10-30#1a.

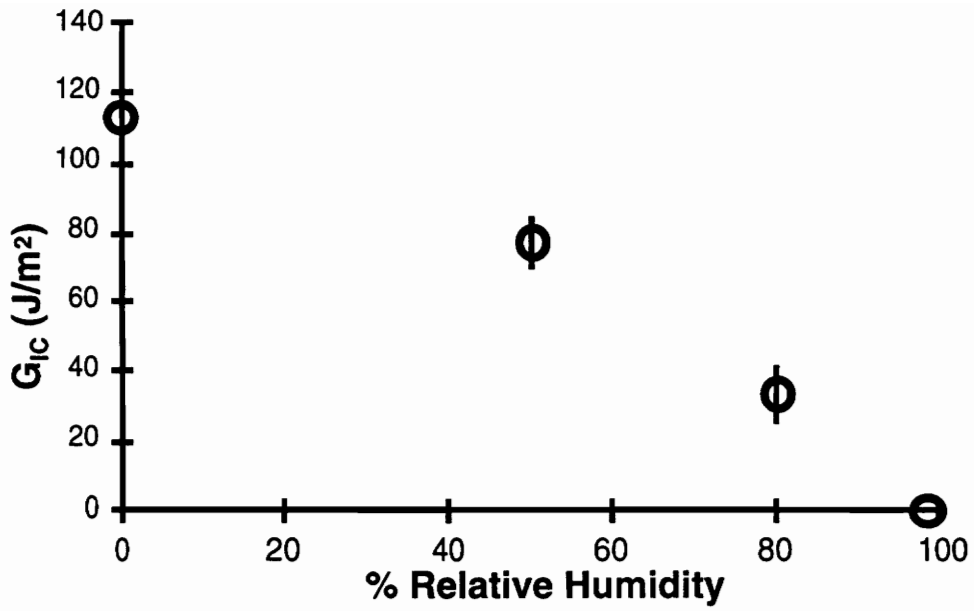

Figure 25. G_{Ic} versus percent relative humidity determined from conditioned DCB tests. (The error bars are ± one standard error from the mean.)

4.7 Discussions

Both NCA and DCB tests on durability show similar trends on the reduction of SERR as the conditioning percent humidity levels increased. It is clear that results obtained from NCA tests are much higher than the results from DCB tests. It is believed that the mixed mode nature of the NCA test was the cause of this difference. It has been widely reported that specimens tend to fail at much lower strain energy release rate values in mode I than in mode II[29]. That is, for every material system, there is a G_{Ic}, and a G_{IIc}; and G_{IIc} tends to be about two to three time higher than G_{Ic}[48]. Since the loading angle, ω, is known for the NCA test, the **G** can be broken down to its modes I and II components. If only the G_I component of NCA tests are used to compare to DCB's G_{Ic} data, the result shows a very good agreement (Fig.26). Currently, it is accepted that G_{IIc} is normally higher than G_{Ic}, so the NCA test results are expected to be higher than the DCB test results, but it is not clear if G_C can be broken down into the different mode components, and then ignoring mode II. In comparing the NCA and the DCB data, the author assumed that such practice can be conducted. Further studies are needed to verify this assumption.

It is known that DCB test results tend to be conservative since mode I is the only loading mode. The majority of practical adhesive joints used in industry are designed to support mixed mode I and II type of loading. The NCA test is a mixed mode test and could be more similar to practical joints. DCB test results had lower standard error values than the NCA results. There are two hypothesis for this phenomenon. The NCA tests were conducted at the early stages of the technique's development; as the technique matured over the period of time, the author was able to lower the scatter. Later test results did show better agreement between replicas. The other explanation for high NCA standard error was that to analyze NCA results, accurate data

on residual stresses and moduli are required. Such information is hard to obtain confidently. For DCB analysis on the other hand, no knowledge of residual stresses is needed, and the effective modulus can be easily determined from analysis.

An important feature in this comparative test of durability was that the total time spent on fabricating, conditioning and testing NCA specimens was about a month while for DCB, the whole process took fifteen months. Besides being time consuming, the cost for conducting DCB tests was also higher. Although the NCA test's monetary advantages were not documented, the amount of steel and adhesive used for DCB was greater, the machining was more costly, and DCB tests required more sophisticated loading frames and data acquisition systems. Overall, NCA tests seemed to be an inexpensive and accelerated test for screening adhesive systems' durability.

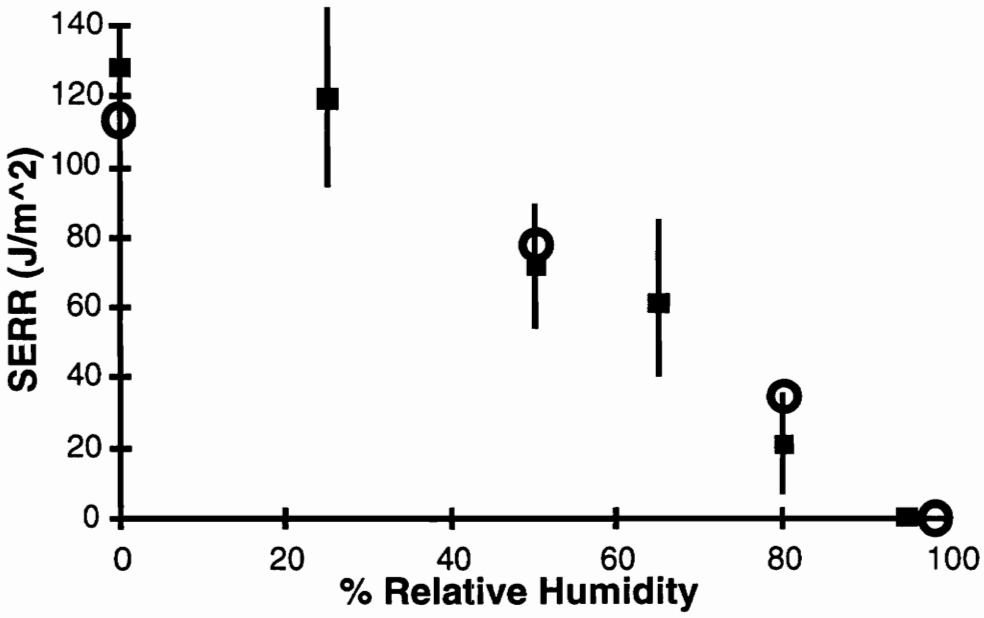

Figure 26. G_{Ic} versus percent relative humidity for both NCA (■) and DCB (O) experiments. (The error bars are ± one standard error from the mean.)

5.0 OTHER APPLICATIONS

Besides accelerated durability tests, the NCA testing method was used for a diverse range of coating adhesion systems to determine the feasibility and the limitations of the test. Coatings studied included structural adhesives, elastomers and waterborne epoxies. The substrate varied from steel, aluminum, titanium and low density polyethylene. Sometimes the surface treatment was altered to study the surface treatment effects, and other times, the thickness was changed to study deformation effects.

5.1 Surface Studies with Ti/LaRC PETI-5

Proper surface treatment is essential for a good adhesive bond. The nearly two dimensional boundaries between the substrate and the adhesive has to hold one another and be able to transfer the applied stresses. The appropriate surface treatment can vary according to the material, environment and application. Sometimes the type of surface treatments can be predicted, but ultimately, the ideal surface preparation is decided from the results of actual experiments.

Not many experiments are designed to generate failure at the interface. It is true that some studies show that when a double cantilever beam (DCB) specimen is loaded slowly, failure tends to be interfacial[41], but this cannot be expected of all adhesive systems. Due to the mode I loading geometry, DCB tests have a tendency to drive the crack into the adhesive. It is only when the interface is very weak relative to the adhesive that the instability drives the crack into the interface. DCB tests can be purposely made to fail interfacially, but this involves changing the load angle to a sliding load mode which is not an easy task. Wedge tests often result in interfacial failures because the

specimens are often exposed to high levels of moisture causing the interphase to weaken, but this may not be guaranteed. If the desired knowledge is on surface treatment effects on an adhesive bond when not exposed to humidity, the wedge test is not a good option. End notched flexure or end notched cantilever tests are quantitative methods to generate interfacial failure and are possible options to study surface treatment effects[49-50].

Because of the loading mode mix, NCA specimens tend to fail interfacially, making the testing method a good tool to quantitatively study surface treatment effects. A series of tests were conducted with the same substrate and coating, but with three different types of surface treatments. The substrate used was titanium Ti-6Al-4V (Ti) with dimensions of 100 x 25.4 x 1.78 mm. The coating was a 0.16 mm thick film of glass scrim cloth supported LaRC PETI-5 adhesive. This adhesive is a high performance thermoplastic polyimide structural adhesive. To fabricate the NCA specimen, an adhesive film with the same dimensions as the titanium was placed between the surface treated substrate and a sheet of Teflon. The system was cured in a hot press at a constant pressure of 516 KPa. After the temperature was ramped at 5.5°C/min. to 350°C, it was held constant for 1 hour, and then lowered back to room temperature at 15°C/min. After cure was completed, the Teflon sheet was removed.

Three types of surface treatment were studied. The first one was to soak the substrate in 1% (v/w) solution of amine propyl trimethoxy silane. This treatment is hereafter referred as silane treatment. The other surface treatment was an alumina grit blast followed by plasma treatment with PEEK. This treatment is referred as PEEK treatment. The last set of specimens was alumina grit blasted and cleaned with acetone. This set of specimens were referred as grit blasted specimens.

Because LaRC PETI-5 is a stiff polymer, to generate the cut and initial debond, a saw blade was used first to saw the polymer apart. Then a razor blade was inserted and tapped into the polymer-substrate interface to generate initial debonds. The testing procedure was the standard procedure described in Section 3.0. Figure (27) shows the critical energy release rate without considering the effects of residual stresses. The residual stresses were not considered because it was assumed that the stresses would be the same for all three types of surface treatments, hence, it can be ignored in a comparative test. Since the failure was interfacial, the difference in adhesive strength could be assumed to be caused by the different surface treatments. The grit blasted specimens were clearly the weakest. The silane treated specimens appear to be the strongest followed closely by the PEEK treated specimens. The results offer adhesive researchers a valuable clue to what surface treatment is the best for their applications. DCB tests on the same adhesive system resulted in a strain energy release rate of 2396±192 J/m^2. All DCB specimens failed cohesively; therefore, little surface treatment effects could determined, and the results could not be compared with the NCA test results.

5.2 Plastic Deformation Experiments

Experiments were conducted to study the plastic deformation of both the coating and the substrate to confirm the analytical predictions. The substrate yielding was predicted to have no significant effect on the results. For the coating, it was thought that as long as only the elastic strain was used to estimate strain energy release rate, the amount of plastic deformation is not important. The system used to study the effect of coating's plastic deformation was a Kapton™ pressure sensitive tape bonded to 1018 mild steel. The Kapton™ tape was 5.83×10^{-5} meters thick. Due to the fact that the tape had a carefully controlled thickness, it offered an excellent thickness

control to the specimen, and it was easy to fabricate. The substrate was wiped with generous amounts of acetone, then the tape was applied to the steel. Several layers of the tape was applied on top of one another until the desired thickness was reached; the specimens tested had thickness varying from 5.83 x 10^{-5} to 3.5 x 10^{-4} mm. A razor blade was used to cut the tape and generate the initial debond; the specimen was tested immediately at a crosshead speed of 15 mm/min.

To determine the mechanical behavior of the Kapton tape, six layers of the tape was bonded on top of each other and tested in the Instron at 15 mm/min. The modulus was determined to be 1.075 GPa. The stress-strain loading history was plotted (Fig. 28). This figure was used to separate the critical strain into plastic and elastic strains. For instance, if critical strain was 0.15, its equivalent coating stress (point A in Fig. 28) was located in the stress-strain curve. The specimen was then unloaded at point A until the stress curve approaches the strain-intercept. The strain from zero to this intercept is the plastic strain, and the strain to the right of the intercept to the critical strain is the elastic strain. To estimate G_C, only the elastic strain was used (in Eq. 3-5) because the energy spent to yield the coating is lost in the process. Figure 29 is G_C plotted against the amount of the coating's plastic deformation which was controlled by changing the thickness of the coating. All experimental data points were plotted, and the line was the linear regression of these points. The results show large amounts of scatter, and the regression line has a slight negative slope. The scatter and the negative slope were blamed on many material aspects of pressure sensitive tapes not accounted for in this study such as viscous dissipation. Statistically speaking however, at 95% confidence level, there is no correlation between plastic deformation and G_C. During the NCA tests, both the load and the strain were recorded and plotted. Since the load was applied predominantly to the steel, it can be

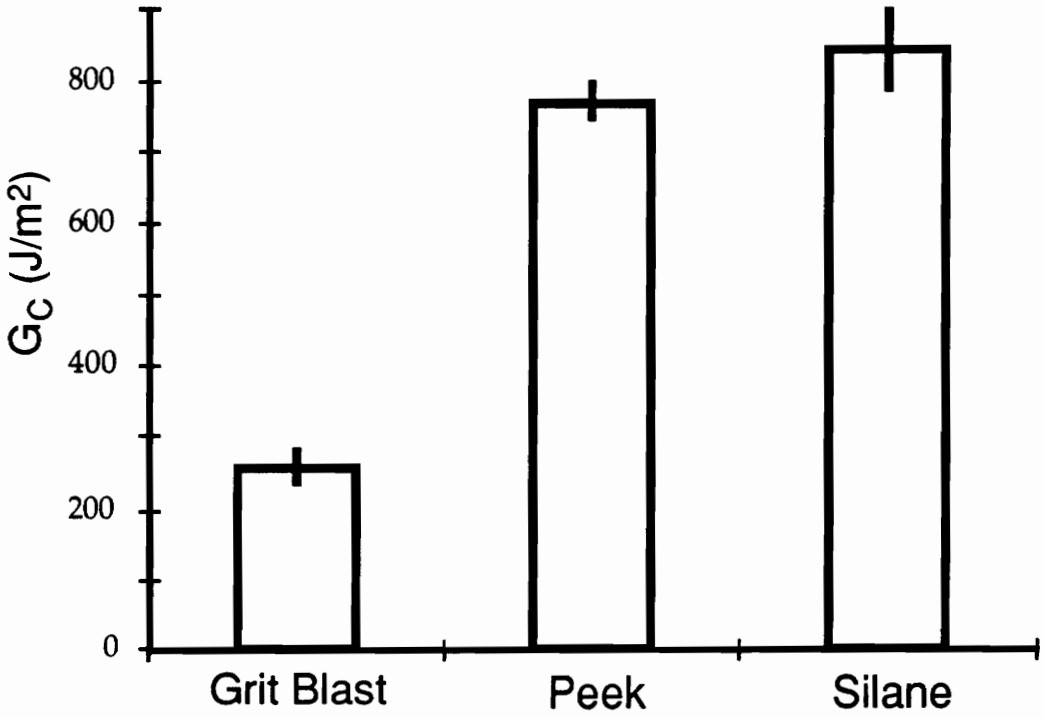

Figure 27. Critical strain energy release rate (G_c) versus three types of surface treatments for Ti/LaRC PETI-5. (The error bars are ± one standard error from the mean).

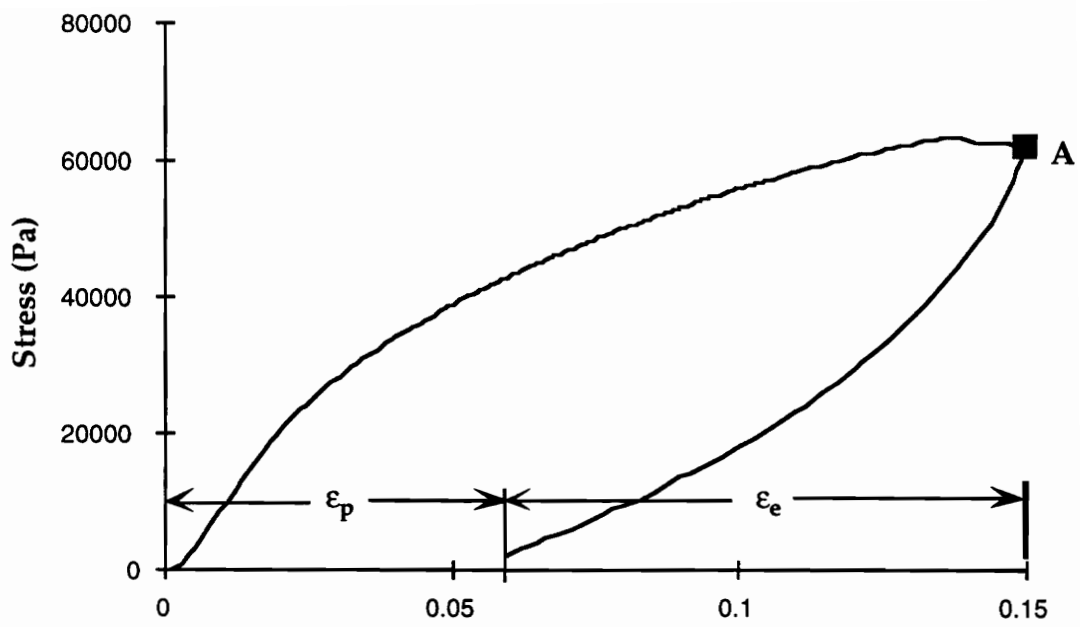

Figure 28. Stress-strain of the Kapton™ tape.

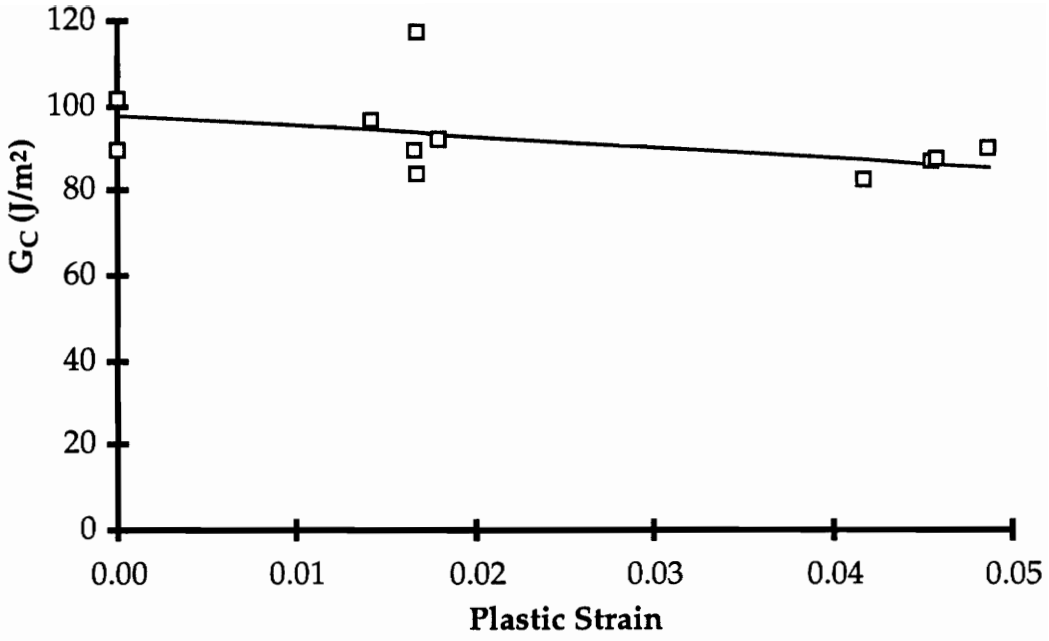

Figure 29. G_C of Kapton™/steel versus plastic strain of the coating.

assumed that the load-strain curve is the loading curve for the substrate, and since mild steel is basically elastic-perfectly plastic material, it was easy to determine the amount of steel's plastic deformation during the test. By varying the thickness of the coating, the critical strain also changed, hence changing the amount of the substrate's plastic deformation. The G_c however, was statistically shown to be unaffected by the coating thickness, the critical strain and the amount of the substrate's plastic deformation.

To further study substrate yielding effects, another experiment was conducted using low density polyethylene (LDPE) substrates bonded to Kapton™ tapes. The other objective of this experiment was to demonstrate the NCA test on polymer coated polymer systems (Dundurs' parameter α of around zero). The dimensions of the substrates were approximately 23 m m by 150 mm by 7 mm. The bonding surfaces were visually inspected, and accepted only if no scratches were found. The surface was then wiped with generous amounts of methanol. The coating was applied immediately after the methanol evaporated. Two layers of the tape applied on top of one another was used, resulting in a thickness of 1.166×10^{-4} m. The NCA test was conducted at a constant cross head speed of 15 mm/min. During the first set of tests, the critical strain always occurred after the substrates had yielded. After the test, the tapes were removed, and the substrates were loaded again, this time well past its yield strain allowing the LDPE substrates to strain harden considerably. Next, two layers of the Kapton™ tapes were once again applied to the substrates and tested. Because of the strain hardening, the substrates had an extended elastic range, and all tapes failed within the elastic range of the substrate. The G_c results for substrates with and without yielding are 32.5 ± 0.58 J/m^2 and 33.9 ± 1.5 J/m^2 respectively. The small difference in the results demonstrated the insignificance of the substrate yielding on the applied **G** in NCA tests.

5.3 Other Experiments

As the world becomes more aware of the need for environmental protection, the adhesive industry is under increased pressure to develop environmentally friendly products. Waterborne adhesives offer the advantage of solvent-free processing; thus, generating a great deal of enthusiasm on the part of the developers. During this early phase of waterborne adhesive development, the NCA test can potentially play a role in screening the new formulations. To demonstrate the NCA test's feasibility, a waterborne epoxy bonded to mild steel system was tested. The epoxy resin was Shell Epi-Rez 3510-W-60 with waterborne curing agent Aquamine 401 produced by Air Products. The specimens were cured at 150°C for 13.5 hours. The thickness of the epoxy varied from 0.5 to 1 mm. The substrate was 1018 mild steel with dimensions of 100 by 12.7 by 2 mm. The specimens were tested at 5 mm/min. Six specimens were tested, and the critical strain energy release rate (G_C) determined was 242±20 J/m^2. The mode mix G_{II}/G_I was found to be 1.7. DCB tests were conducted on a similar waterborne epoxy/steel system. During fabrication, the waterborne epoxy was applied to both DCB substrates; the epoxy was allowed to cure in room conditions until the color of the epoxy turned from white to translucent (approximately 1 hour). The reason for this was to allow water to evaporate before exposing the specimens to high temperatures. At this point the specimens were joined, and placed in an oven at 150° for 60 minutes. The testing procedure for DCB test was described previously, the G_C was estimated to be 105.5±9.65 J/m^2. The DCB results were lower than the NCA results even if only G_I results were compared. A possible explanation for the discrepancy is that the specimens had different curing procedures. Studies with waterborne epoxy DCBs cured with similar conditions are part of the current research efforts in this research group at Virginia Tech. Once these results are obtained, a more significant comparison with the NCA test will be possible.

In another experiment, a commercially available plastic food wrap made of thin polyvinylchloride (PVC) film was attached to polypropylene substrates. The bonding surfaces were visually inspected, and accepted only if no scratches were found. This NCA specimen was used to simulate plastic wrap clinged to Tupperware™. The tests were conducted at 10 mm/min. And the $\mathbf{G_C}$ determined was 0.915±0.029 J/m^2. The Dundurs' parameter α was -0.89, and the mode mix $\mathbf{G_{II}/G_I}$ was found to be 2.18; therefore, $\mathbf{G_I}$ was found to be 0.288±0.009 J/m^2. Peel tests conducted on the same material system[51] resulted in a $\mathbf{G_C}$ of 0.467±0.01 J/m^2. The mode mix $\mathbf{G_{II}/G_I}$ for the peel test was calculated to be 0.46. resulting in a G_I of 0.319 J/m^2. The difference is about 10 percent. The ten percent discrepancy could be due to various data acquisition variances accumulated both from the peel tests and the NCA tests, and also the fact that only $\mathbf{G_I}$ was considered important.

6.0 CONCLUSION

A methodology is presented for estimating coating adhesive performance. The notched coating adhesion (NCA) specimens consist of single substrates coated with thin layers of film. The coating is notched to induce debonds, and the specimen is then loaded in tension. Due to the loading geometry, failure is always interfacial. The strain at which coating debonding occurs is then used to determine the critical strain energy release rate. Detailed specimen fabrication, testing procedure and analysis, both finite element and analytical solutions, were developed. Testing analysis was designed and developed successfully for most combinations of material mismatches.

In the feasibility research, the benefits and the limitations of the NCA test were studied. Experimentally, the NCA test was found to work well with pressure sensitive tapes bonded to various types of substrates, thin polymer films clinged to polymer substrates, and structural adhesives such as epoxy and LaRC-PETI 5 bonded to metals. The test also proved its usefulness in interface and surface treatment studies because of its tendency to cause interfacial failure. An important limitation to the test is that the residual stresses and the moduli must be known in order to accurately determine bond strength; such information is not easy to obtain confidently.

For durability studies, it was demonstrated that by using coated specimens to study interfacial degradation due to moisture yields similar results as the sandwiched specimens. Conventional specimens consisting of two substrates bonded with an adhesive require lengthy exposure times in order to allow humidity to penetrate throughout the bond. A coating specimen in which the adhesive is applied as a coating to a substrate has a shortened diffusion path which greatly reduces the time required to saturate

the bond and interface region. Assuming that bond degradation is diffusion limited, this accelerated conditioning may provide meaningful estimates of bond strength. There are several coating tests, but because of the simple geometry, interfacial failure, quantitative fracture results, and reduced moisture ingression time, the NCA test may be a good candidate to obtain preliminary results on environmental effects in bonded joints. Environmentally conditioned steel/epoxy adhesive systems were tested with both DCB and NCA testing techniques. In addition to being quick and inexpensive, the NCA results correlated well with the DCB results, and if only G_{Ic} was considered, the results were quite similar.

The proposed NCA test is a simple, quick and inexpensive method to quantitatively determine coating adhesion strength. Although not intended to replace conventional adhesion tests, due to its cost effectiveness, the method is believed to have significant potential as a screening test for durability studies and in ensuring user confidence and promoting widespread use of adhesives.

7.0 RECOMMENDATIONS FOR FUTURE WORK

With the ultimate goal of being able to use the NCA test to accurately predict bond durability and interphase effects, some possible research topics to be conducted in the future to refine the testing technique are suggested. Viscoelasticity effects on the NCA test is a possible research topic. It is expected that viscoelasticity affects the NCA test. The viscoelastic analysis may not be involved since if the debond propagation is fast enough, the viscous effect is minimal. A three dimensional finite element analysis could be conducted. This study has the potential of obtaining a better picture to what happens to the specimen when the substrate deforms plastically, and also the width effects on the NCA test could be studied. New research has demonstrated that when polymer/metal joints are thermally cycled, the residual stresses change. Since when NCA specimens fail, the residual stresses are released, it might be a good candidate to study the thermal cycle of polymer/metal joints. NCA specimens tested in fatigue can also be an interesting research topic. When loaded in fatigue, the crack propagation speed can be correlated to the number of loading cycles and maximum loads.

REFERENCE

1. T. Chang, E. A. Sproat, Y. H. Lai, N. E. Shephard and D. A. Dillard, "Testing Methods for Accelerated Humidity Conditioning and Estimation of Adhesive Bond Durability", *J. Adhesion* (in press).

2. M. C. Y. Niu, *Airframe Structural Design: Practical Design Information and Data on Aircraft Structures* (Conmilit Press, Los Angeles, 1988).

3. L. H. Sharpe, "Overview: Adhesives Technology", *Engineered Materials Handbook, Volume 3: Adhesives and Sealants,* H. F. Brinson Ed. (American Society of Material, United States, 1990).

4. S. Kalpakjian, *Manufacturing Engineering and Technology*, (Addison-Wesley Publishing Company, Reading, Massachusetts, 1992).

5. M. Goland and E. Reissner, "Stresses in Cement Joints", *Journal of Applied Mechanics*, **66,** A-17 (1944).

6. M. D. Rakestraw, M. W. Taylor, T. Chang and D. A. Dillard, "Time Dependent Crack Growth and Loading Rate Effects on Interfacial and Cohesive Fracture of Adhesive Joints", *J. Adhesion*, **55**, 123 (1995).

7. A. Gledhill, A. J. Kinloch, and S. J. Shaw, "A Model for Predicting Joint Durability", *J. Adhesion*, **11**, 3 (1980).

8. H. Andrews and A. Stevenson, "Fracture Energy of Epoxy Resin Under Plane Strain Conditions", *J. Materials Science*, **13**, 1680 (1978).

9. G. D. Vaughn, B. G. Frushour and W. C. Dale, "Scratch Indentation, a Simple Adhesion Test Method for Thin Films on Polymeric Supports", *J. Adhesion Sci. Technol.*, **8**, 635 (1994).

10. J. Valli, "A Review of Adhesion Test Methods for Thin Hard Coatings", *J. Vac. Sci. Technol.*, **A4**, 3007 (1986).

11. R. J. Farris and C. L. Bauer, "A Self-Delamination Method of Measuring the Surface Energy of Adhesion of Coatings", *J. Adhesion*, **26**, 293 (1988).

12. M. D Thouless and H. M. Jensen, "Elastic Fracture Mechanics of the Peel-Test Geometry", *J. Adhesion*, **38**, 185 (1992).

13. K. S. Kim and J. Kim, "Elasto-Plastic Analysis of the Peel Test for Thin Film Adhesion", *Engineering Materials and Technology*, **110**, 266 (1988).

14. K. S. Kim and N. Aravas, "Elastoplastic Analysis of the Peel Test", *Int. J. Solids Structures*, **24**, 417 (1988).

15. ASTM, "D3359-93 Standard Test Method for Measuring Adhesion by Tape Test", *Annual Book of ASTM Standards*, 433 (1995).

16. K. R. Cropper and R. J. Young, "The Interlaminar Bond Strength of Flexible Polymer-Metal Laminates", *J. Adhesion*, **34**, 153 (1991).

17. D. A. Dillard and Y. Bao, "The Peninsula Blister Test: A High and Constant Strain Energy Release Rate Fracture Specimen for Adhesives", *J. Adhesion*, **33**, 253 (1991).

18. H. Dannenberg, "Measurement of Adhesion by a Blister Method", *J. Applied Polymer Science*, **5**, 125 (1961).

19. D. W. Butler, C. T. H. Stoddart and P. R. Stuart, "The Stylus or Scratch Method for Thin Film Adhesion Measurement: Some Observations and Comments", *J. Phys.*, **D3**, 877 (1970).

20. U. Helmersson, B. O. Johansson, J. E. Sundgren, H. T. G. Hentzell and P. Billgren, "Adhesion of Titanium Nitride Coatings on High-Speed Steel", *J. Vac. Sci. Technol.* **A3**, 308 (1985).

21. W. J. O'Kane and R. J. Young, "Interlaminar Bond Strength and Failure Mechanisms in Commercial Flexible Polymer-Metal Laminates", *J. Adhesion*, **41**, 203 (1993).

22. Y. H. Lai and D. A. Dillard, "A Study of the Fracture Efficiency Parameter of Blister Tests for Films and Coatings", *J. Adhesion Sci. Technol*, **8**, 663 (1994).

23. W. Althof, "The Influence of Moisture on Adhesive Bonded Joints", *Adhesion 5*, K. W. Allen, Ed. 15 (Applied Science Publishers, Barking, Essex, 1980).

24. J. Comyn, D. M. Brewis, and S. T. Tredwell, "Bonding of Aluminum Alloy with Some Phenolic Adhesives and a Modified Epoxide Adhesive, and Strength Changes on Exposure to Moist Air at 50°C", *J. Adhesion*, **21**, 59 (1987).

25. J. Cognard, "Environmental Attack on Adhesive Joints Studied by Cleavage Fracture", *J. Adhesion*, **26**, 155 (1988).

26. J. Cognard, "Quantitative Measurement of the Energy of Fracture of an Adhesive Joint Using the Wedge-Test", *J. Adhesion*, **22**, 97 (1987).

27. ASTM, "D3433-75, Standard Practice for Fracture Strength in Cleavage of Adhesives in Bonded Joints", *Annual Book of ASTM Standards*, 299 (1984).

28. D. Broek, *Elementary Engineering Fracture Mechanics* (Martinus Nijhoff Publishers, Dordrecht, Netherlands, 1986).

29. M. F. Kanninen and C. H. Popelar, *Advanced Fracture Mechanics* (Oxford University Press, New York, 1985).

30. J. E. Ritter, T. J. Lardner, L. Rosenfeld and M. R. Lin, "Measurement of Adhesion of Thin Polymer Coatings by Indentation", *J. Appl. Phys.*, **66**, 3626 (1989).

31. T. R. Brussat, S. T Chiu and S. Mostovoy, *Fracture Mechanics for Structural Adhesive Bonds*, AFNL-TR-77-163 (Air Force Materials Laboratory, Wright-Patterson AFB, Ohio, 1977).

32. Y. H. Lai, M. D. Rakestraw and D. A. Dillard, "Cracked Lap Shear Specimen Revisited-A Closed Form Solution", *International Journal of Solids and Structures*, **33**, 1725 (1996).

33. W. S. Johnson, "Stress Analysis of the Cracked Lap Shear Specimen: an ASTM Round Robin", *ASTM J. Testing and Evaluation*, **8**, 663 (1987).

34. J. W. Hutchinson and Z. Suo, "Mixed Mode Cracking in Layered Material", *Advances in Applied Mechanics*, **29**, 63 (1992).

35. H. M. Jensen, J. W. Hutchinson, and K. S. Kim, "Decohesion of a Cut Prestressed Film on a Substrate", *Int. J. Solids and Structures*, **26**, 1099 (1990).

36. Z. Suo and J. W. Hutchinson, "Sandwich Test Specimens for Measuring Interface Crack Toughness", *Materials Science and Engineering*, **A107**, 135 (1989).

37. Y. H. Lai and D. A. Dillard, "Using the Fracture Efficiency to Compare Adhesion Tests", *International Journal of Solids and Structures*, (in press).

38. ABAQUS 5.4 Software, Hibbitt, Karlsson & Sorensen, Inc. (1994).

39. C. E. Knight, personal communication, professor of Mechanical Engineering, Virginia Tech (Aug. 1995).

40. A. G. Evans, M. D. Drory and M. S. Hu, "The Cracking and Decohesion of Thin Films", *J. Mater. Res.* **3**, 1043 (1988).

41. M. D. Rakestraw, M. A. Vrana, T. Chang, D. A. Dillard, T. C. Ward and J. G. Dillard, *Evaluation of Adhesive Performance Using Static, Fatigue, and Environmental Fracture Testing* (Center for Adhesive and Sealant Science, Blacksburg, 1994).

42. ASTM, "D5032-90, Standard Practice for Maintaining Constant Relative Humidity by Means of Aqueous Glycerin Solutions", *Annual Book of ASTM Standards*, 451 (1990).

43. D. R. Lefebvre, K. M. Takahashi, A. J. Muller and V. R. Raju, "Degradation of Epoxy Coatings in Humid Environments: The Critical Relative Humidity for Adhesion Loss", *J. Adhesion Sci. Technol.* **5**, 201 (1991).

44. J. Comyn, "The Relationship Between Joint Durability and Water Diffusion", *Adhesion*, **6**, K. W. Allen, Ed., 279 (Applied Science Publishers, Barking, Essex, 1981).

45. J. Comyn, "Kinetics and Mechanism of Environmental Attack", *Durability of Structural Adhesives*, A. J. Kinloch, Ed., 85 (Applied Science Publishers, Barking, Essex, 1983).

46. J. Crank and G. S. Park, *Diffusion in Polymers* (Academic Press, London, 1968).

47. F. A. Kamke, personal communication, professor of Wood Science and Forest Products, Virginia Tech (Aug. 1994).

48. G. P. Anderson, S. J. Bennett and K. L. DeVries, *Analysis and testing of Adhesive Bonds* (Academic Press, New York, 1977).

49. A. J. Russell and K. N. Street, "Moisture and Temperature Effects on the Mixed-Mode Delamination Fracture of Unidirectional Graphite/Epoxy",

Delamination and Debonding of Materials, W. S. Johnson Ed. (ASTM STP 876, 1985).

50. N. J. Pagano, *Interlaminar Response of Composite Materials* (Elsevier, Amsterdam, 1989).

51. C. L. Randow, personal communication, graduate student in Engineering Mechanics, Virginia Tech (March 1996).

APPENDIX A

The following is the NCA two dimensional finite element model written for ABAQUS 5.4 software. The code is written to be post processed with ABAQUS Post 5.4.

```
*HEADING
NCA 2D WITH SINGULAR ELEMENTS
**
**************************************************************
**       Modeling of NCA specimen
**
**Two dimensional analysis of NCA specimen
**Half of the specimen modeled
**Length = 40 mm
**Coating thickness = 0.15 mm
**Substrate thickness = 2 mm
**Crack at 5 mm from the tip
**Coating: Epoxy, modulus = 2.970 GPa,
**Poisson's ratio = 0.4.
**Substrate: Steel, modulus = 203 GPa,
** Poisson's ratio = 0.3, yield stress= 200 MPa.
**Displacement strain = 0.025
**3 J-Integral contours around crack tip
**************************************************************
**
**Assign nodes at the corners
**
*NODE
**LEFT
1,0.,-2.
2,0.,-1.
3,0.,-0.15
4,0.,-0.1
5,0.,-0.065
6,0.,-0.055
7,0.,-0.045
8,0.,-0.035
9,0.,-0.025
10,0.,-0.01875
11,0.,-0.0125
12,0.,-0.00625
13,0.,0.
14,0.,0.00625
15,0.,0.0125
16,0.,0.01875
```

```
17,0.,0.025
18,0.,0.035
19,0.,0.045
20,0.,0.055
21,0.,0.065
22,0.,0.1
23,0.,0.15
**
**MID
438,34.96,-2.
439,34.96,-1.
440,34.96,-0.15
441,34.96,-0.1
442,34.96,-0.065
443,34.96,-0.055
444,34.96,-0.045
445,34.96,-0.035
446,34.96,-0.025
447,34.96,-0.01875
448,34.96,-0.0125
449,34.96,-0.00625
450,34.96,0.
451,34.96,0.00625
452,34.96,0.0125
453,34.96,0.01875
454,34.96,0.025
455,34.96,0.035
456,34.96,0.045
457,34.96,0.055
458,34.96,0.065
459,34.96,0.1
460,34.96,0.15
**
**MID1
461,34.975,-2.
462,34.975,-1.
463,34.975,-0.15
464,34.975,-0.1
465,34.975,-0.065
466,34.975,-0.055
467,34.975,-0.045
468,34.975,-0.035
469,34.975,-0.025
470,34.975,-0.01875
471,34.975,-0.0125
472,34.975,-0.00625
473,34.975,0.
474,34.975,0.
475,34.975,0.00625
476,34.975,0.0125
477,34.975,0.01875
```

```
478,34.975,0.025
479,34.975,0.035
480,34.975,0.045
481,34.975,0.055
482,34.975,0.065
483,34.975,0.1
484,34.975,0.15
**
**MID2
653,35.025,-2.
654,35.025,-1.
655,35.025,-0.15
656,35.025,-0.1
657,35.025,-0.065
658,35.025,-0.055
659,35.025,-0.045
660,35.025,-0.035
661,35.025,-0.025
662,35.025,-0.01875
663,35.025,-0.0125
664,35.025,-0.00625
665,35.025,0.
666,35.025,0.
667,35.025,0.00625
668,35.025,0.0125
669,35.025,0.01875
670,35.025,0.025
671,35.025,0.035
672,35.025,0.045
673,35.025,0.055
674,35.025,0.065
675,35.025,0.1
676,35.025,0.15
**
**RIGHT
893,40.,-2.
894,40.,-1.
895,40.,-0.15
896,40.,-0.1
897,40.,-0.065
898,40.,-0.055
899,40.,-0.045
900,40.,-0.035
901,40.,-0.025
902,40.,-0.01875
903,40.,-0.0125
904,40.,-0.00625
905,40.,0.
906,40.,0.
907,40.,0.00625
908,40.,0.0125
```

```
909,40.,0.01875
910,40.,0.025
911,40.,0.035
912,40.,0.045
913,40.,0.055
914,40.,0.065
915,40.,0.1
916,40.,0.15
**
**Nodes around singular elements
1000,35.,0.
1224,35.,0.
1006,35.025,0.
1034,35.025,0.025
1090,34.975,0.025
1146,34.975,-0.025
1202,35.025,-0.025
1230,35.025,0.
**
**Generate node sets
*NSET,NSET=LEFT,GENERATE
1,23
*NSET,NSET=MID,GENERATE
438,460
*NSET,NSET=MID1,GENERATE
461,484
*NSET,NSET=MID2,GENERATE
653,676
*NSET,NSET=RIGHTSUB,GENERATE
893,905
*NSET,NSET=RIGHTADH,GENERATE
906,916
*NSET,NSET=RIGHT,GENERATE
893,916
*NGEN,NSET=TIP
1000,1224,7
*NGEN,NSET=OUTER
1006,1034,7
1034,1090,7
1090,1146,7
1146,1202,7
1202,1230,7
*NFIL,BIAS=1.5
LEFT,MID,19,23
*NFIL,BIAS=0.5
MID2,RIGHT,10,24
*NFIL
MID1,MID2,8,24
*NFIL,SINGULAR=1
TIP,OUTER,6,1
**
```

```
**Define elements
*ELEMENT,TYPE=CPE8R
**Define left corner elements
1,1,47,49,3,24,48,26,2
111,461,509,511,463,485,510,487,462
127,480,528,530,482,504,529,506,481
139,701,749,751,703,725,750,727,702
201,13,59,61,15,36,60,38,14
401,714,762,764,716,738,763,740,715
**
**Define elements around singular elements
531,421,467,1146,423,444,468,446,422
532,467,515,1160,1146,491,516,1153,468
533,515,563,1174,1160,539,564,1167,516
534,563,611,1188,1174,587,612,1181,564
535,611,659,1202,1188,635,660,1195,612
536,659,707,709,1202,683,708,685,660
537,1202,709,711,1216,685,710,687,1209
538,1216,711,713,1230,687,712,689,1223
539,423,1146,1132,425,446,1139,448,424
540,425,1132,1118,427,448,1125,450,426
541,427,1118,1104,429,450,1111,452,428
542,429,1104,1090,431,452,1097,454,430
543,1006,714,716,1020,690,715,692,1013
544,1020,716,718,1034,692,717,694,1027
545,431,1090,480,433,454,479,456,432
546,1090,1076,528,480,1083,527,504,479
547,1076,1062,576,528,1069,575,552,527
548,1062,1048,624,576,1055,623,600,575
549,1048,1034,672,624,1041,671,648,623
550,1034,718,720,672,694,719,696,671
**
**Define elements under singular elements
801,415,461,463,417,438,462,440,416
802,417,463,465,419,440,464,442,418
803,419,465,467,421,442,466,444,420
804,653,701,703,655,677,702,679,654
805,655,703,705,657,679,704,681,656
806,657,705,707,659,681,706,683,658
**
**Define elements above singular elements
807,433,480,482,435,456,481,458,434
808,435,482,484,437,458,483,460,436
809,672,720,722,674,696,721,698,673
810,674,722,724,676,698,723,700,675
**
**Define first singular element
300,1000,1002,1016,1014,1001,1009,1015,1007
**
**Generate elements in substrate
*ELGEN
```

```
300,3,2,1,16,14,3
*ELGEN,ELSET=SUBSTRATE
1,9,46,1,6,2,9
111,4,48,1,3,2,4
139,4,48,1,6,2,4
*ELSET,ELSET=SUBSTRATE,GENERATE
801,806
531,540
324,347
**
**Generate elements in coating
*ELGEN,ELSET=ADHESIVE
201,9,46,1,5,2,9
127,4,48,1,2,2,4
401,4,48,1,5,2,4
*ELSET,ELSET=ADHESIVE,GENERATE
541,550
807,810
300,323
**
**Define material properties
*MATERIAL,NAME=STEEL
*ELASTIC,TYPE=ISOTROPIC
203E3,0.3
*PLASTIC
200.,0.
265.,0.0004
*MATERIAL,NAME=EPOXY
*ELASTIC,TYPE=ISOTROPIC
2970.,0.4
*SOLID SECTION,ELSET=SUBSTRATE,MATERIAL=STEEL
*SOLID SECTION,ELSET=ADHESIVE,MATERIAL=EPOXY
**
**Define boundary and loading conditions
*BOUNDARY
LEFT,1,2
RIGHTSUB,2,2
*STEP
*STATIC
*BOUNDARY
RIGHTSUB,1,1,1.0
*J-INTEGRAL,CONTOURS=3
0.0,1.0
TIP
**
**Output
*NODE PRINT
U
*RESTART,WRITE
*END STEP
```

APPENDIX B

The NCA test was originally developed for accelerated durability studies. In the beginning of the durability studies it was decided that since diffusion time nominally varies as the square of the diffusion distance, there was a need to have a reduced specimen size for accelerated conditioning. Coating specimens seemed the best choice for this task since water diffused through the thickness of the coating. Several test methods, both old and new were attempted to quantitatively evaluate accelerated durability of coating adhesives. NCA was identified as the best testing method for this purpose, but there are some other testing methods evaluated that offered similar potential if properly developed or if some specific type of adhesive system is used.

This section describes some of the testing methods that were attempted; the successes and the failures. The reader may use this section as a guide to develop some of the ideas presented in the section and to learn from the mistakes.

For all testing methods studied, the substrate used was 1018 steel, the adhesive was rubber toughened epoxy. The system is the same as that described in section 4.1.

B.1 Blister Test

One of the potential accelerated durability tests is the blister test. There are many types of blister tests and the peninsula blister test[17] was chosen for this study. In the test, the strain energy release rate is independent of the crack length. Although the constrained blister test also proves to be a constant strain energy release rate test, the specimen size for the peninsula

blister test is smaller. Furthermore, with the peninsula blister test, the fracture efficiency is higher, *i.e.*, high energy release rates are possible with low pressures. The equation to determine strain energy release rate is derived as[16]:

$$G = \frac{P^2}{1440Db}\left[16a^5 - (a-b)^5\right] \qquad \text{(B1)}$$

Where G is strain energy release rate;

P is applied pressure;

D is plate rigidity;

2a is total fixture width, and

2b is peninsula width.

It has been demonstrated that the peninsula blister test works well with some soft polymer films attached to metal substrates with pressure sensitive adhesives, but the goal of the experiment was for the test to work for stiff adhesives such as epoxy. Unfortunately, the specimen fabrication with the epoxy/steel system was difficult, and experiments did not move past the fabrication process.

To fabricate a peninsula blister specimen, there must a U shaped debond from which pressure can be applied. Mechanical removal of the substrate to form a U shaped hole was abandoned since it was uncertain if this would affect the bonded region of the specimen. Efforts were directed at finding a mask that would prevent adhesive exposure to the steel in the desired debonded area. After several attempts with Kapton tape, Teflon sheet, magnetized thin steel shim, and release agent spray no success was obtained. Even if success was obtained with the generation of the U shaped debonded area, potentially, the epoxy would need to be reinforced to increase toughness so that it would not fracture during the blister test. To summarize, blister

tests could be good for accelerated durability studies on flexible coatings and films that have a weak bond; However, for stiff materials, and strong bonds, it is probably not a good option.

B.2 Modified Double Cantilever Beam Test

Modified DCB tests were attempted to study accelerated durability of the epoxy/steel system. In a conventional DCB test, the specimens are fabricated by curing the adhesive to both substrates. In this experiment procedure, a thin layer of adhesive was cured to a single steel substrate. The specimens were conditioned in humidity chambers until 90% saturation was achieved. By using thin adhesive layers, the time needed to equilibrate the specimens was short. After equilibrating the specimens, both the cured adhesive layer and the second steel substrate were sandblasted and treated with a primer (1% solution of aminopropyl-triethoxysilane in ethanol). The adhesive surfaces were then bonded with TruBond 2-Ton epoxy. To insure the crack propagated along the conditioned interface, a pre-crack was introduced. Unfortunately, all conditioned specimens failed during specimen preparation after humidity conditioning. All failures appeared to be interfacial along the coating and the substrate. The failure was attributed to the weak bond between the epoxy and the steel after the humidity degradation. The testing method appeared to show good potential for systems with strong bonds and high modulus. The method of bonding the second substrate to the specimen after humidity conditioning can potentially be applied to other types of sandwich tests such as single lap joints, wedge tests and inverse peel tests.

B.3 Modified Notched Coating Adhesion Test

Besides loading in tension, the proposed NCA specimen can be loaded in bending (Fig. B1). The specimen is bent on different molds of increasing radius of curvature. At a critical radius of curvature, the stress becomes high enough to cause the adhesive to debond; the resulting critical strain energy release rate is

$$G = \frac{h}{2\hat{E}}\left[\left(\sigma_t + \sigma_m + \frac{y\hat{E}}{\rho}\right)^2 + \left(\sigma_t + \sigma_m - \frac{y\upsilon\hat{E}}{\rho}\right)^2\right] \qquad \text{(B2)}$$

where y is the distance of the interface from the neutral axis, and

ρ is the critical radius of curvature.

All the NCA specifications, preparations and fabrications described in the paper apply to this type of loading. Since the bending is usually performed manually, the substrate and the adhesive have to be flexible enough for manual bending or bending with the aid of a vise. The advantage of loading in bend is that there is no need for axial loading frames, and extensometers. This makes the bending test even more cost effective, and the results should still be acceptable. Because of the bending effect, the degree of mode mix changes, and Eq. (6) is no longer valid. The bending NCA test is a good substitute of the conventional NCA testing when resources are limited, and many established coating tests can conceivably be used as accelerated humidity tests. These include the scratch indentation test, the peel tests and the cross-hatch tape test. For the epoxy/steel system studied, the NCA test was determined to be the best test; however, for other systems, both the blister test and the modified DCB test may also be suitable candidates for quantitative accelerated durability tests.

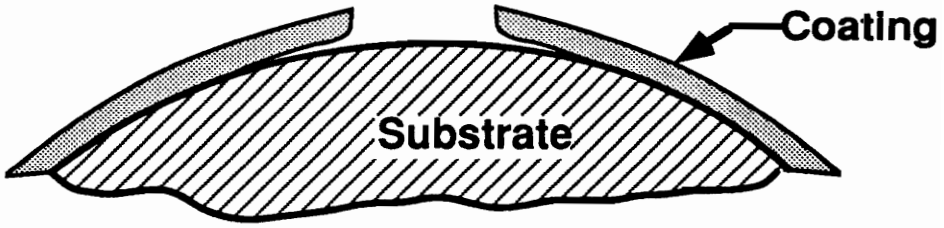

Figure B1. The debond of a NCA specimen under bending.

VITA

Tsunou Chang was born on October 2, 1970 in Taipei, Taiwan. At the age of 10 he moved to Brazil. In 1989 he started his undergraduate studies at Virginia Tech in Aerospace Engineering. His senior design project was the winner of the AIAA's National Collegiate Airplane Design Competition which about 100 teams participated. After graduating in August 1993, the author started graduate school in Materials Science and Engineering at the same university. After receiving the Master of Science degree in May 1996, Tsunou will work for Graco Inc. in Plymouth, Michigan.